

Dark matter in the scale-invariant 3-3-1-1 model

Alex G. Dias,¹ Kristjan Kannike,^{2,*} Niko Koivunen,^{2,†} Julio Leite,^{3,‡} Vinicius Padovani,^{1,§} and B. L. Sánchez-Vega^{4,¶}

¹*Centro de Ciências Naturais e Humanas, Universidade Federal do ABC, 09210-580, Santo André-SP, Brasil*

²*National Institute of Chemical Physics and Biophysics, Rävala 10, 10143, Tallinn, Estonia*

³*AHEP Group, Institut de Física Corpuscular – C.S.I.C./Universitat de València, Parc Científic de Paterna. C/ Catedrático José Beltrán, 2 E-46980 Paterna (Valencia) - Spain*

⁴*Departamento de Física, UFMG, Belo Horizonte, MG 31270-901, Brasil.*

(Dated: January 31, 2025)

We propose a scale-invariant model with the 3-3-1-1 gauge symmetry that features universal seesaw for all fermion masses. The discrete remnant of the gauge group, the matter parity, stabilizes a fermionic dark matter candidate. The scalar sector contains two triplets, the minimum number to break the 3-3-1 symmetry, and two scalar singlets.

With the help of additional vector-like quarks, the universal implementation of the seesaw mechanism across all fermion sectors provides a partial explanation for the observed hierarchy of masses for charged leptons, neutrinos, and quarks.

We identify the lightest P_M -odd fermion, f_d , as a viable dark matter candidate. This fermion satisfies the relic density constraint and the spin-independent constraints within the mass range $160 \text{ GeV} \lesssim m_{f_d} \lesssim 520 \text{ GeV}$. This range depends on the symmetry-breaking scale v_χ with a lower bound $v_\chi \gtrsim 3.6 \text{ TeV}$ due to LEP bounds on the ρ_0 parameter. Spin-independent scattering cross-sections for f_d align with experimental limits from LZ and PandaX-4T, with some regions of the parameter space nearing the sensitivity of upcoming experiments, such as XLZD and PandaX-xT, which offers promising opportunities for detection.

* Kristjan.Kannike@cern.ch

† niko.koivunen@kbfi.ee

‡ julio.leite@ific.uv.es

§ vinipadovani@alumni.usp.br

¶ bruce@fisica.ufmg.br

CONTENTS

I. Introduction	3
II. The Scale-invariant 3-3-1-1 Model	4
III. Scalar Sector	7
A. Scalar Potential	7
B. Potential Minimum and P_M -even Mass Matrix	8
C. P_M -odd Sector	11
IV. Perturbative Unitarity	11
V. Gauge Sector	13
VI. Yukawa Sector: Seesaw-Suppressed Fermion Masses	15
A. Lepton Spectrum	16
1. Charged Leptons	16
2. Neutrinos	17
3. Dark Leptons	18
B. Quark Spectrum	19
1. Up-type Quarks	20
2. Down-type Quarks	21
VII. Bounds from Charged Leptons	22
VIII. Dark Matter	24
IX. Conclusions	29
Acknowledgments	31
References	32

I. INTRODUCTION

The enormous success of the Standard Model (SM) has still left unanswered quite a few questions, such as neutrino mass, dark matter (DM), and the number of fermion families. The last question finds an answer in the family of 3-3-1 models, which have been extensively studied in the literature [1–10]. One of the most notable features of these models is that the number of fermion families must be a multiple of three due to the non-trivial nature of anomaly cancellation. Additionally, these models exhibit a rich structure enabling the incorporation of new particles that can address other open problems of the SM, such as the dark matter puzzle, the strong CP problem, and the origin of neutrino masses [11–17].

We propose a model with dynamical symmetry breaking based on the gauge group $SU(3)_C \otimes SU(3)_L \otimes U(1)_X \otimes U(1)_N$ that extends the 3-3-1 gauge group by an additional $U(1)$ symmetry [12–16]. The $SU(3)_C$ represents the color symmetry of the Standard Model, $SU(3)_L$ extends the left-handed chirality symmetry, and $U(1)_X$ and $U(1)_N$ are a combination of charge and $B - L$.

One of the driving forces behind the proposed model is the reduction in the number of scalar fields in high representations of the gauge group and the free parameters in the scalar potential, especially those with mass dimension, when compared to the original 3-3-1 models. These parameters tend to make the models less predictive and introduce scalar complexity that, in some cases, becomes excessive compared to other extensions of the SM, such as the two-Higgs-doublet model (see [18]) and the minimal supersymmetric standard model (see [19]). For instance, in the original 3-3-1 models, the scalar sector includes an enlarged set of nontrivial $SU(3)_L$ multiplets of scalar fields, such as three triplets [1, 4–10] and, in some cases, three triplets plus a sextet [3].

In order to achieve a very compact and more predictive scalar sector, we follow the same strategy as in [20]. Specifically, we introduce the minimal number of triplets required to dynamically break the gauge symmetry to $SU(3)_C \otimes U(1)_Q$ via the Coleman-Weinberg mechanism [21] in the Gildener-Weinberg approximation [22]. The minimal number of triplets needed to achieve this is two. However, as first discussed in [11], despite these two triplets breaking the gauge symmetry, accidental chiral symmetries typically remain. These symmetries are usually associated with generators that are combinations of the diagonal generators of $SU(3)_L$ and a Peccei-Quinn-like symmetry, as shown in [23].

As it happens, this symmetry is also chiral in the quark sector (and occasionally in the lepton sector), leaving some particles massless. This situation is inconsistent with experimental observations. Therefore, the accidental symmetry must be broken to generate mass terms for these particles. To address this issue,

we introduce new vector-like quarks and leptons.

At first glance, this might seem like a mere translation of the complexity from the scalar sector to the fermion sector. However, there are several advantages to this approach. The first is that these new fermions can be used to implement a universal see-saw mechanism [24], which partially addresses the hierarchy of fermion masses—an unresolved issue in the Standard Model. Moreover, these fermions acquire masses at an energy scale related to scale invariance, which in this model is significantly higher than the electroweak and 3-3-1 scales due to the requirements of the see-saw mechanism. As a result, the number of physical degrees of freedom at the TeV scale becomes smaller and more manageable, making the model more feasible for phenomenological studies.

As a benefit of the extended gauge group, the matter parity that stabilizes DM arises as a discrete remnant symmetry from the symmetry breaking [12, 14, 20, 25–30]. While we have several potential dark matter candidates, only a dark fermion f_d can satisfy the direct detection constraints.

We systematically explore the key aspects of the proposed model. In Section II, we present the details of the model, including the gauge group and field content. Section III focuses on the scalar sector, detailing the scalar potential, vacuum structure, and mass spectrum. In Section IV, we examine perturbative unitarity constraints, deriving bounds on the quartic couplings and other parameters of the model. Section V discusses the gauge boson sector, highlighting the mass spectrum and the role of the Z'' boson in stabilizing the scalar potential. The Yukawa sector is analyzed in Section VI, where we demonstrate how the seesaw mechanism generates the masses of fermions, including charged leptons, neutrinos, and quarks. In Section VII, we explore experimental constraints from charged lepton processes, and in Section VIII, we provide a detailed analysis of the dark matter phenomenology, identifying the fermion f_d as a viable candidate. Finally, the main results are summarized in the conclusions IX.

II. THE SCALE-INVARIANT 3-3-1-1 MODEL

Although we follow the same general strategy as in [20], there are some important differences in both the symmetry structure and the field content. To be more specific, we choose to introduce the η triplet (instead of $\rho = (\rho_1^+, \rho_2^0, \rho_3^+)^T \sim (1, 3, 2/3)$) and the χ triplet, which transform under the $SU(3)_C \otimes SU(3)_L \otimes U(1)_X \otimes U(1)_N$ group as $(1, 3, -1/3, 1/3)$ and $(1, 3, -1/3, -2/3)$, respectively.

In other words,

$$\eta = \left(\eta_1^0 \equiv \frac{v_\eta + S_{\eta_1} + iA_{\eta_1}}{\sqrt{2}}, \eta_2^-, \eta_3^0 \right)^T, \quad \chi = \left(\chi_1^0, \chi_2^-, \chi_3^0 \equiv \frac{v_\chi + S_{\chi_3} + iA_{\chi_3}}{\sqrt{2}} \right)^T. \quad (1)$$

Note that η and χ transform differently under the $U(1)_N$ symmetry. This is an important point because we require that η_1^0 and χ_3^0 acquire vacuum expectation values (VEVs) in order to break the gauge symmetry down to $SU(3)_C \otimes U(1)_Q$. If these fields transformed identically under all the gauge groups, a gauge rotation could be performed to set one of the VEVs to zero.

As usual, we also embed the SM quarks and leptons in the representations:

$$L_{iL} = (\nu_i, e_i, f_i)_L^T, \quad Q_{aL} = (d_a, -u_a, D_a)_L^T, \quad Q_{3L} = (u_3, d_3, U_3)_L^T, \quad (2)$$

where $a = 1, 2, i = 1, 2, 3$, and L_{iL} , Q_{aL} , and Q_{3L} transform under the gauge group $SU(3)_C \otimes SU(3)_L \otimes U(1)_X \otimes U(1)_N$ as $(1, 3, -1/3, -2/3)$, $(3, \bar{3}, 0, 0)$, and $(3, 3, 1/3, 2/3)$, respectively. As previously mentioned, the two scalar triplets η and χ in Eq. (1) are not enough to generate masses for all the quarks and leptons. Thus, we introduce vector-like fermions $\mathcal{F}_{iL,R}$, $\mathcal{K}_{aL,R}$, and $\mathcal{K}_{3L,R}$:

$$\mathcal{F}_{iL,R} = (E_i, -f'_i, E'_i)_{L,R}^T, \quad \mathcal{K}_{aL,R} = (\mathcal{U}_a, \mathcal{D}_a, \mathcal{U}'_a)_{L,R}^T, \quad \mathcal{K}_{3L,R} = (\mathcal{D}_3, -\mathcal{U}_3, \mathcal{D}'_3)_{L,R}^T, \quad (3)$$

in order to allow terms such as $\overline{L_{iL}} \eta^* \mathcal{F}_{jR}$, $\overline{\mathcal{F}_{iL}} \chi^* e_{jR}$, $\overline{Q_{aL}} \eta \mathcal{K}_{bR}$ and $\overline{Q_{3L}} \eta^* \mathcal{K}_{3R}$ which ensure that all the SM fermions become massive, the fields $\mathcal{F}_{iL,R}$, $\mathcal{K}_{aL,R}$ and $\mathcal{K}_{3L,R}$ have to belong to $(1, \bar{3}, -2/3, -1/3)$, $(3, 3, 1/3, -1/3)$ and $(3, \bar{3}, 0, 1)$ representation of the 3-3-1-1 gauge group.

However, it is still necessary to introduce a new real singlet scalar,

$$\varphi = \frac{v_\varphi + S_\varphi}{\sqrt{2}} \sim (1, 1, 0, 0), \quad (4)$$

to give masses for the $\mathcal{F}_{iL,R}$, $\mathcal{K}_{aL,R}$, and $\mathcal{K}_{3L,R}$ through terms such as $\varphi \overline{\mathcal{F}_{iL}} \mathcal{F}_{jR}$, $\varphi \overline{\mathcal{K}_{aL}} \mathcal{K}_{bR}$ and $\varphi \overline{\mathcal{K}_{3L}} \mathcal{K}_{3R}$.

Although the lepton triplet L_{iL} in Eq. (2) contains ν_{iL} , the gauge symmetries do not allow neutrino masses as in the Standard Model. To address this, we introduce right-handed neutrinos $\nu_{iR} \sim (1, 1, 0, -1)$, motivated by current oscillation experiments, which require at least two neutrinos to be massive and necessarily non-degenerate. Together with the introduction of a complex scalar field

$$\sigma = \frac{v_\sigma + S_\sigma + iA_\sigma}{\sqrt{2}} \sim (1, 1, 0, 2), \quad (5)$$

this allows the implementation of a type-I see-saw mechanism [31–35]. Note that σ is the only field responsible for breaking the $U(1)_N$ symmetry and for giving mass to the neutral gauge boson associated with that symmetry.

Fields	3-3-1-1	Q	B-L	P_M -Parity
L_{iL}	$1, 3, -1/3, -2/3$	$(0, -1, 0)^T$	$(-1, -1, 0)^T$	$(+, +, -)^T$
e_{iR}	$1, 1, -1, -1$	-1	-1	$+$
Q_{aL}	$3, \bar{3}, 0, 0$	$(-1/3, 2/3, -1/3)^T$	$(1/3, 1/3, -2/3)^T$	$(+, +, -)^T$
Q_{3L}	$3, 3, 1/3, 2/3$	$(2/3, -1/3, 2/3)^T$	$(1/3, 1/3, 4/3)^T$	$(+, +, -)^T$
u_{iR}	$3, 1, 2/3, 1/3$	$2/3$	$1/3$	$+$
d_{iR}	$3, 1, -1/3, 1/3$	$-1/3$	$1/3$	$+$
ν_{iR}	$1, 1, 0, -1$	0	-1	$+$
f_{iR}	$1, 1, 0, 0$	0	0	$-$
$\mathcal{F}_{iL,R}$	$1, \bar{3}, -2/3, -1/3$	$(-1, 0, -1)^T$	$(0, 0, -1)^T$	$(-, -, +)^T$
U_{3R}	$3, 1, 2/3, 4/3$	$2/3$	$4/3$	$-$
D_{aR}	$3, 1, -1/3, -2/3$	$-1/3$	$-2/3$	$-$
$\mathcal{K}_{aL,R}$	$3, 3, 1/3, -1/3$	$(2/3, -1/3, 2/3)^T$	$(-2/3, -2/3, 1/3)^T$	$(-, -, +)^T$
$\mathcal{K}_{3L,R}$	$3, \bar{3}, 0, 1$	$(-1/3, 2/3, -1/3)^T$	$(4/3, 4/3, 1/3)^T$	$(-, -, +)^T$
η	$1, 3, -1/3, 1/3$	$(0, -1, 0)^T$	$(0, 0, 1)^T$	$(+, +, -)^T$
χ	$1, 3, -1/3, -2/3$	$(0, -1, 0)^T$	$(-1, -1, 0)^T$	$(-, -, +)^T$
σ	$1, 1, 0, 2$	0	2	$+$
φ	$1, 1, 0, 0$	0	0	$+$

TABLE I. Summary of fermion and scalar fields, their representations under the gauge group $SU(3)_C \otimes SU(3)_L \otimes U(1)_X \otimes U(1)_N$, electric charges (Q), $B-L$ charges, and their transformations under the dark parity P_M symmetry. The fields that do not contain any SM particles are marked red.

Regarding gauge symmetries, this model shares most of its features with the rest of the 3-3-1 models. Specifically, the choice of the field representations under the $SU(3)_C \otimes SU(3)_L \otimes U(1)_X$ symmetry is determined by anomaly cancellation, the allowance of tree-level mass generation, and ensuring that the SM fermions have the correct electric charges. It is also important to note that the $U(1)_X$ charges are chosen such that no quarks possess exotic electric charges. The electric charge operator Q is defined as:

$$Q = T_3 - \frac{1}{\sqrt{3}}T_8 + X \mathbf{1}_{3 \times 3}, \quad (6)$$

where T_3 and T_8 are the diagonal generators of $SU(3)_L$.

Moreover, the representation of the fields under $U(1)_N$ is chosen such that the SM fermions have the conventional $B-L$ charges, and a discrete symmetry

$$P_M = (-1)^{3(B-L)+2s}, \quad (7)$$

where s is the spin of the fields, remains after spontaneous symmetry breaking [12, 14, 20, 25–30]. Here, $B - L$ is defined as:

$$B - L = -\frac{2}{\sqrt{3}}T_8 + N \mathbf{1}_{3 \times 3}, \quad (8)$$

For example, in the particular case of the $U(1)_N$ charge for the L_{iL} triplet, it should be chosen as $-2/3$. A summary of all the fields and their representations under the gauge group is provided in Table I.

The P_M symmetry stabilizes several neutral fields that can, in principle, serve as candidates for dark matter. Finally, we note that a neutral fermion charged under the P_M symmetry, $f_{iR} \sim (1, 1, 0, 0)$, is introduced to also implement a see-saw mechanism in the DM leptonic sector.

III. SCALAR SECTOR

In this section, we study the scalar sector at tree level, as it plays a crucial role in understanding dynamical symmetry breaking. Additionally, it allows us to determine the mass eigenstates in different sectors, which we primarily classify as CP-even and CP-odd. In this model, the CP-odd sector is also P_M -odd. The P_M -odd sector refers to scalars that are non-trivially charged under the P_M symmetry, which, in principle, stabilizes the dark matter sector. Due to our consideration that all quartic coupling constants and vacuum expectation values are real, these sectors do not mix with each other. The charged scalar sector in this model is rather straightforward, as all charged fields, $(\eta_2^-, \chi_2^-, \eta_2^+, \chi_2^+)$, exhibit a mass matrix that is identically zero. Consequently, these fields correspond to Nambu-Goldstone bosons, which are subsequently absorbed by the respective charged gauge fields.

A. Scalar Potential

Let us consider the most general renormalizable, scale-invariant scalar potential that preserves the gauge symmetry of the model:

$$\begin{aligned} V_0 = & \lambda_\chi (\chi^\dagger \chi)^2 + \lambda_\eta (\eta^\dagger \eta)^2 + \lambda_{\eta\chi} (\chi^\dagger \chi) (\eta^\dagger \eta) + \lambda'_{\eta\chi} (\chi^\dagger \eta) (\eta^\dagger \chi) \\ & + \lambda_{\chi\varphi} (\chi^\dagger \chi) \varphi^2 + \lambda_{\chi\sigma} (\chi^\dagger \chi) (\sigma^* \sigma) + \lambda_{\eta\varphi} (\eta^\dagger \eta) \varphi^2 + \lambda_{\eta\sigma} (\eta^\dagger \eta) (\sigma^* \sigma) \\ & + \lambda_\varphi \varphi^4 + \lambda_\sigma (\sigma^* \sigma)^2 + \lambda_{\varphi\sigma} (\sigma^* \sigma) \varphi^2. \end{aligned} \quad (9)$$

Since the potential V_0 is biquadratic in the fields, it can be conveniently expressed as:

$$V_0 = (\Phi^{\circ 2})^T \Lambda(\theta) \Phi^{\circ 2}, \quad (10)$$

where the vector of field norms $(\Phi^{\circ 2})^T \equiv (|\eta|^2, |\chi|^2, |\sigma|^2, |\varphi|^2) \geq 0$, the symmetric matrix

$$\Lambda(\theta) = \begin{pmatrix} \lambda_\eta & \frac{1}{2}(\lambda_{\eta\chi} + \lambda'_{\eta\chi}\theta) & \frac{1}{2}\lambda_{\eta\sigma} & \frac{1}{2}\lambda_{\eta\varphi} \\ \star & \lambda_\chi & \frac{1}{2}\lambda_{\chi\sigma} & \frac{1}{2}\lambda_{\chi\varphi} \\ \star & \star & \lambda_\sigma & \frac{1}{2}\lambda_{\varphi\sigma} \\ \star & \star & \star & \lambda_\varphi \end{pmatrix} \quad (11)$$

contains quartic couplings, and the orbit parameter $\theta \equiv (\chi^\dagger\eta)(\eta^\dagger\chi)/(|\eta|^2|\chi|^2) \in [0, 1]$ due to the Cauchy–Schwartz inequality. Notice here that we are using the Hadamard product, defined as the element-wise product, e.g. $[(A)^{\circ 2}]_{ij} = a_{ij}^2$ for a matrix A with elements a_{ij} .

B. Potential Minimum and P_M -even Mass Matrix

We proceed to calculate the mass eigenvalues and eigenstates of the CP-even sector. To do this, we must first find the minimum of the scalar potential. Following standard procedures, we expand V_0 in terms of the fields $(\Phi^{\circ 2})^T = \frac{1}{2}(S_{\eta 1}^2, S_{\chi 3}^2, S_\sigma^2, S_\varphi^2)$, which acquire VEVs, while setting all other fields to zero. Additionally, we work within the Gildener-Weinberg approximation [22], which allows us to calculate the effective potential perturbatively along the flat direction, as this method is convenient for models with multiple scalar fields. Moreover, as we will see in Eq. (25), $\lambda'_{\eta\chi}$ is positive, ensuring that, at the minimum of the potential, the orbit parameter θ equals zero. In other words, at the minimum $V_0(\Phi) = (\Phi^{\circ 2})^T \Lambda(\theta = 0) \Phi^{\circ 2} \equiv (\Phi^{\circ 2})^T \Lambda \Phi^{\circ 2}$, where, for simplicity, we denote $\Lambda \equiv \Lambda(0)$.

To explicitly determine the flat direction, described by $\Phi = \xi \mathbf{n}$, where ξ represents the radial degree of freedom (the dilaton) and \mathbf{n} is a unit vector, we proceed following [36]. The central idea is to minimise the potential $V_0(\Phi) = (\Phi^{\circ 2})^T \Lambda \Phi^{\circ 2}$, subject to the condition $V_0(\mathbf{n}) = 0$. As shown in detail in Ref. [36], the Hadamard square of the unit vector \mathbf{n} is an eigenvector of the quartic coupling matrix Λ with a null eigenvalue, given by

$$\mathbf{n}^{\circ 2} = \frac{\text{adj}(\Lambda)e}{e^T \text{adj}(\Lambda)e}. \quad (12)$$

Here, $\text{adj}(\Lambda)$ is the adjugate matrix of Λ , defined as $\Lambda \text{adj}(\Lambda) = \det(\Lambda)I$, the vector $e = (1, \dots, 1)^T$ on the respective space has all elements equal to unity, and I is the identity matrix. The condition $V_0(\mathbf{n}) = 0$ is guaranteed by taking $\det(\Lambda) = 0$, as seen by inserting Eq. (12) in Eq. (10).

The 1-loop effective potential along the flat direction is given by (see [20, 21, 36, 37])

$$V^{1\text{-loop}}(\xi\mathbf{n}) = B(\mathbf{n})\xi^4 \left(\ln \frac{\xi^2}{v_\xi^2} - \frac{1}{2} \right), \quad (13)$$

where ξ is the dilaton field, $v_\xi \equiv \sqrt{v_\eta^2 + v_\chi^2 + v_\sigma^2 + v_\varphi^2}$ its VEV, and

$$B(\mathbf{n}) = \frac{1}{64\pi^2 v_\xi^4} \left(\sum_S m_S^4 + 3 \sum_V m_V^4 - 4 \sum_F m_F^4 \right) \quad (14)$$

is the sum over all degrees of freedom.

The mass matrix for the CP-even fields that get VEVs can be written as¹

$$M_\Phi^2 = v_\xi^2 \nabla_{\mathbf{N}}^T \nabla_{\mathbf{N}} V(\mathbf{N})|_{\mathbf{N}=\mathbf{n}} = 2\Lambda \circ (\mathbf{nn}^T) v_\xi^2, \quad (15)$$

where \mathbf{N} is a unit vector in the Φ direction. Solving Eq. (15) for the quartic coupling matrix Λ , we get

$$\Lambda = \frac{1}{2v_\xi^2} M_\Phi^2 \circ (\mathbf{nn}^T)^{\circ-1}, \quad (16)$$

where $(\mathbf{nn}^T)^{\circ-1}$ means the element-wise inverse, i.e. $[(\mathbf{nn}^T)^{\circ-1}]_{ij} = 1/(n_i n_j)$ in Hadamard notation.

Eq. (16) is particularly useful as it enables us to express the quartic couplings in terms of the tree-level scalar masses, the VEVs, and mixing angles. To illustrate this, let us define the diagonal mass matrix $M_{\text{CP-even}}^2$ for the CP-even fields that acquire VEVs as $M_{\text{CP-even}}^2 = \text{diag}(m_{H_1}^2, m_{H_2}^2, m_{H_3}^2, m_{H_4}^2)$, which is related to M_Φ^2 by

$$M_\Phi^2 = O M_{\text{CP-even}}^2 O^T, \quad (17)$$

where the orthogonal matrix O is given by [38, 39]

$$O = O_{34} O_{24} O_{14} O_{23} O_{13} O_{12}. \quad (18)$$

Each O_{ij} defines a rotation in the ij -plane; we denote the mixing angle in O_{ij} as α_{ij} and also abbreviate $s_{ij} \equiv \sin \alpha_{ij}$ and $c_{ij} \equiv \cos \alpha_{ij}$.

Considering $m_{H_4} = m_\xi = 0$ as the dilaton mass at tree level, we have the last column of O as the flat direction:

$$\mathbf{n} = \left(s_{14} \quad c_{14}s_{24} \quad c_{14}c_{24}s_{34} \quad c_{14}c_{24}c_{34} \right)^T. \quad (19)$$

¹ Note that due to normalisation of the fields, the numerical coefficient on the right-hand side is different from Ref. [36].

Thus, the quartic couplings can be expressed in terms of the VEVs, CP-even scalar masses, and mixing angles using Eq. (16). Here, we note that the angles in Eq. (19), $\alpha_{14}, \alpha_{24}, \alpha_{34}$, can be easily written in terms of the VEVs as

$$\alpha_{14} = \arctan \left(\frac{v_\eta}{\sqrt{v_\chi^2 + v_\sigma^2 + v_\varphi^2}} \right), \quad \alpha_{24} = \arctan \left(\frac{v_\chi}{\sqrt{v_\sigma^2 + v_\varphi^2}} \right), \quad \alpha_{34} = \arctan \left(\frac{v_\sigma}{v_\varphi} \right). \quad (20)$$

The remaining angles in Eq. (18), α_{12}, α_{13} , and α_{23} , cannot be expressed only in terms of the VEVs. However, they are strongly constrained by the perturbative unitarity conditions and the hierarchy in the VEVs, $v_\eta \ll v_\chi \ll v_\sigma, v_\varphi$ arising from the imposition of the see-saw mechanism throughout the fermion sector. In this model, it is natural to identify v_η with the Standard Model VEV, $v_{\text{SM}} = 246.22$ GeV, since the W^\pm mass, as shown in Eq. (37), is entirely determined by v_η . Thus, we identify the mass eigenstate H_1 as the SM-like Higgs with mass $m_{H_1} = 125.11$ GeV. The H_2 eigenstate acquires a mass at the 331-breaking scale, v_χ . Finally, the H_3 eigenstate acquires a mass at the scale of v_σ and v_φ , leading to the hierarchy $m_{H_1} \ll m_{H_2} \ll m_{H_3}$. The dilaton H_4 obtains a mass at one-loop level: it is given by

$$m_{H_4}^2 = 8B(\mathbf{n})v_\xi^2. \quad (21)$$

For the SM-like Higgs $H_1 \approx S_{\eta 1}$, it is required that $\alpha_{12} \approx 0$. Additionally, to keep the couplings within the perturbative regime, the angles α_{13} and α_{23} must be small. To derive useful expressions for the CP-even eigenstates, we set these angles to zero. Under this approximation, we have:

$$\begin{aligned} H_1 &= \frac{(v_\chi^2 + v_\sigma^2 + v_\varphi^2)S_{\eta 1} - v_\eta(v_\chi S_{\chi 3} + v_\varphi S_\varphi) - v_\eta v_\sigma S_\sigma}{\sqrt{(v_\sigma^2 + v_\varphi^2)(v_\eta^2 + v_\sigma^2 + v_\varphi^2)}} \approx S_{\eta 1}, \\ H_2 &= \frac{(v_\sigma^2 + v_\varphi^2)S_{\chi 3} - v_\chi(v_\sigma S_\sigma + v_\varphi S_\varphi)}{\sqrt{(v_\eta^2 + v_\sigma^2 + v_\varphi^2)(v_\eta^2 + v_\chi^2 + v_\sigma^2 + v_\varphi^2)}} \approx S_{\chi 3}, \\ H_3 &= \frac{v_\varphi S_\sigma - v_\sigma S_\varphi}{\sqrt{(v_\sigma^2 + v_\varphi^2)}}, \\ H_4 &= \frac{v_\eta S_{\eta 1} + v_\chi S_{\chi 3} + v_\sigma S_\sigma + v_\varphi S_\varphi}{\sqrt{(v_\eta^2 + v_\chi^2 + v_\sigma^2 + v_\varphi^2)}} \approx \frac{v_\sigma S_\sigma + v_\varphi S_\varphi}{\sqrt{(v_\sigma^2 + v_\varphi^2)}}. \end{aligned} \quad (22)$$

Actually, we need to have small non-zero values for the angles α_{12} , α_{13} and α_{23} to allow non-zero couplings of the fermion DM candidate to scalar field in order to ensure the correct relic density.

C. P_M -odd Sector

Finally, we focus our attention on the calculation of the P_M scalar sector. In the basis, $B_d = (\eta_3, \chi_1^*)^T$, the P_M -odd mass matrix is

$$M_d^2 = \begin{pmatrix} \frac{1}{2}\lambda'_{\eta\chi}v_\chi^2 & \frac{1}{2}\lambda'_{\eta\chi}v_\eta v_\chi \\ \frac{1}{2}\lambda'_{\eta\chi}v_\eta v_\chi & \frac{1}{2}\lambda'_{\eta\chi}v_\eta^2 \end{pmatrix}. \quad (23)$$

The matrix M_d is diagonalized by the orthogonal transformation $O_d^T M_d^2 O_d = \text{diag}(m_{G_d}, m_{S_d})$, where

$$O_d = \begin{pmatrix} -\frac{v_\eta}{\sqrt{v_\chi^2 + v_\eta^2}} & \frac{v_\chi}{\sqrt{v_\chi^2 + v_\eta^2}} \\ \frac{v_\chi}{\sqrt{v_\chi^2 + v_\eta^2}} & \frac{v_\eta}{\sqrt{v_\chi^2 + v_\eta^2}} \end{pmatrix}. \quad (24)$$

Its eigenvalues are $m_{G_d}^2 = 0$ for a dark Goldstone and $m_{S_d}^2 = \frac{1}{2}(v_\eta^2 + v_\chi^2)\lambda'_{\eta\chi}$ for a physical dark mass eigenstate S_d . We can now find the $\lambda'_{\eta\chi}$ parameter:

$$\lambda'_{\eta\chi} = \frac{2m_{S_d}^2}{(v_\eta^2 + v_\chi^2)}. \quad (25)$$

The dark scalar mass eigenstates are given by

$$\begin{aligned} G_d &= -\frac{v_\eta}{\sqrt{v_\chi^2 + v_\eta^2}}\eta_3 + \frac{v_\chi}{\sqrt{v_\chi^2 + v_\eta^2}}\chi_1^*, \\ S_d &= \frac{v_\chi}{\sqrt{v_\chi^2 + v_\eta^2}}\eta_3 + \frac{v_\eta}{\sqrt{v_\chi^2 + v_\eta^2}}\chi_1^*. \end{aligned} \quad (26)$$

Note that the scalar S_d can, in principle, act as a dark matter candidate.

IV. PERTURBATIVE UNITARITY

Perturbative unitarity constraints arise from the requirement that the scattering matrix be unitary, ensuring the conservation of probability in particle interactions, and are explored by analyzing the tree-level two-to-two scattering amplitudes dominated by quartic interactions in the high-energy limit $\sqrt{s} \rightarrow \infty$. In this context, the eigenvalues \mathcal{T}^{ba} of the scattering matrix must satisfy the condition $\Re(\mathcal{T}_0^{ba}) \leq \frac{1}{2}$ for the theory to remain perturbatively unitary.

At the zeroth partial wave order, in the high-energy limit, the matrix element can be expressed as [40]:

$$\mathcal{T}_0^{ba} = \frac{1}{16\pi} \frac{1}{\sqrt{2^{\delta_{s_1, s_2}} 2^{\delta_{s_3, s_4}}}} \frac{\partial V_0}{\partial S_1 \partial S_2 \partial S_3^* \partial S_4^*} \Big|_n \leq \frac{1}{2}, \quad (27)$$

where a corresponds to the initial state $S_1 + S_2$ and b to the analogous final state $S_3 + S_4$ for the two-to-two scattering process.

By calculating the scattering matrix for all possible two-to-two initial and final states, including Goldstone bosons, we derive constraints on the quartic couplings. These constraints are given by:

$$\begin{aligned}
|\lambda_\eta| &\leq 4\pi, & |\lambda_{\eta\sigma}| &\leq 8\pi, & |\lambda_{\eta\varphi}| &\leq 8\pi, & |\lambda_\sigma| &\leq 4\pi, & |\lambda_\chi| &\leq 4\pi, \\
|\lambda_\eta - \sqrt{\lambda_\eta^2 - 2\lambda_\eta\lambda_\chi + \lambda'_{\eta\chi}{}^2 + \lambda_\chi^2} + \lambda_\chi| &\leq 8\pi, \\
|\lambda_\eta + \sqrt{\lambda_\eta^2 - 2\lambda_\eta\lambda_\chi + \lambda'_{\eta\chi}{}^2 + \lambda_\chi^2} + \lambda_\chi| &\leq 8\pi, \\
|\lambda_{\eta\chi} - \lambda'_{\eta\chi}| &\leq 8\pi, & |\lambda_{\chi\sigma}| &\leq 8\pi, & |\lambda_{\chi\varphi}| &\leq 8\pi, \\
|\lambda_{\eta\chi}| &\leq 8\pi, & |\lambda'_{\eta\chi} + \lambda_{\eta\chi}| &\leq 8\pi, & |3\lambda'_{\eta\chi} + \lambda_{\eta\chi}| &\leq 8\pi.
\end{aligned} \tag{28}$$

Additionally, the four solutions λ_i to the following quartic equation must satisfy $|\lambda_i| \leq 4\pi$:

$$\lambda^4 + \lambda^3 A + \lambda^2 B + \lambda C + D = 0, \tag{29}$$

with coefficients explicitly given as

$$A = -\frac{1}{2}(8\lambda_\eta + 4\lambda_\sigma + 3\lambda_\varphi + 8\lambda_\chi), \tag{30}$$

$$\begin{aligned}
B = \frac{1}{8} \left(-64\lambda_\eta\lambda_\sigma - 48\lambda_\eta\lambda_\varphi - 128\lambda_\eta\lambda_\chi + 6\lambda_{\eta\sigma}^2 + 3\lambda_{\eta\varphi}^2 + 2\lambda_{\chi\eta}'^2 + 12\lambda_{\chi\eta}'\lambda_{\chi\eta} \right. \\
\left. - 24\lambda_\sigma\lambda_\varphi - 64\lambda_\sigma\lambda_\chi - 48\lambda_\varphi\lambda_\chi + \lambda_{\varphi\sigma}^2 + 18\lambda_{\chi\eta}^2 + 6\lambda_{\chi\sigma}^2 + 3\lambda_{\chi\varphi}^2 \right),
\end{aligned} \tag{31}$$

$$\begin{aligned}
C = \frac{1}{8} \left(9\lambda_{\eta\sigma}^2\lambda_\varphi - 96\lambda_\eta\lambda_\sigma\lambda_\varphi + \lambda_{\chi\eta}'^2(4\lambda_\sigma + 3\lambda_\varphi) + 4\lambda_\eta\lambda_{\varphi\sigma}^2 + 24\lambda_{\eta\sigma}^2\lambda_\chi - 256\lambda_\eta\lambda_\sigma\lambda_\chi - 192\lambda_\eta\lambda_\varphi\lambda_\chi \right. \\
- 96\lambda_\sigma\lambda_\varphi\lambda_\chi + 4\lambda_{\varphi\sigma}^2\lambda_\chi + 6\lambda_{\eta\varphi}^2(\lambda_\sigma + 2\lambda_\chi) + 36\lambda_\sigma\lambda_{\chi\eta}^2 + 27\lambda_\varphi\lambda_{\chi\eta}^2 - 18\lambda_{\eta\sigma}\lambda_{\chi\eta}\lambda_{\chi\sigma} \\
+ 24\lambda_\eta\lambda_{\chi\sigma}^2 + 9\lambda_\varphi\lambda_{\chi\sigma}^2 - 3\lambda_{\varphi\sigma}\lambda_{\chi\sigma}\lambda_{\chi\varphi} + 12\lambda_\eta\lambda_{\chi\varphi}^2 + 6\lambda_\sigma\lambda_{\chi\varphi}^2 + 3\lambda_{\chi\eta}'(8\lambda_\sigma\lambda_{\chi\eta} \\
+ 6\lambda_\varphi\lambda_{\chi\eta} - 2\lambda_{\eta\sigma}\lambda_{\chi\sigma} - \lambda_{\eta\varphi}\lambda_{\chi\varphi}) - 3\lambda_{\eta\varphi}(\lambda_{\eta\sigma}\lambda_{\varphi\sigma} + 3\lambda_{\chi\eta}\lambda_{\chi\varphi}),
\end{aligned} \tag{32}$$

$$\begin{aligned}
D = \frac{1}{32} (\lambda_{\chi\eta}'^2(-24\lambda_\sigma\lambda_\varphi + \lambda_{\varphi\sigma}^2) - 96\lambda_{\eta\varphi}^2\lambda_\sigma\lambda_\chi - 144\lambda_{\eta\sigma}^2\lambda_\varphi\lambda_\chi + 1536\lambda_\eta\lambda_\sigma\lambda_\varphi\lambda_\chi \\
+ 48\lambda_{\eta\sigma}\lambda_{\eta\varphi}\lambda_{\varphi\sigma}\lambda_\chi - 64\lambda_\eta\lambda_{\varphi\sigma}^2\lambda_\chi - 216\lambda_\sigma\lambda_\varphi\lambda_{\chi\eta}^2 + 9\lambda_{\varphi\sigma}^2\lambda_{\chi\eta}^2 + 108\lambda_{\eta\sigma}\lambda_\varphi\lambda_{\chi\eta}\lambda_{\chi\sigma} - 18\lambda_{\eta\varphi}\lambda_{\varphi\sigma}\lambda_{\chi\eta}\lambda_{\chi\sigma} \\
+ 9\lambda_{\eta\varphi}^2\lambda_{\chi\sigma}^2 - 144\lambda_\eta\lambda_\varphi\lambda_{\chi\sigma}^2 + 72\lambda_{\eta\varphi}\lambda_\sigma\lambda_{\chi\eta}\lambda_{\chi\varphi} - 18\lambda_{\eta\sigma}\lambda_{\varphi\sigma}\lambda_{\chi\eta}\lambda_{\chi\varphi} - 18\lambda_{\eta\sigma}\lambda_{\eta\varphi}\lambda_{\chi\sigma}\lambda_{\chi\varphi} \\
+ 48\lambda_\eta\lambda_{\varphi\sigma}\lambda_{\chi\sigma}\lambda_{\chi\varphi} + 9\lambda_{\eta\sigma}^2\lambda_{\chi\varphi}^2 - 96\lambda_\eta\lambda_\sigma\lambda_{\chi\varphi}^2 - 6\lambda_{\chi\eta}'(24\lambda_\sigma\lambda_\varphi\lambda_{\chi\eta} - \lambda_{\varphi\sigma}^2\lambda_{\chi\eta} - 6\lambda_{\eta\sigma}\lambda_\varphi\lambda_{\chi\sigma} \\
+ \lambda_{\eta\varphi}\lambda_{\varphi\sigma}\lambda_{\chi\sigma} - 4\lambda_{\eta\varphi}\lambda_\sigma\lambda_{\chi\varphi} + \lambda_{\eta\sigma}\lambda_{\varphi\sigma}\lambda_{\chi\varphi}).
\end{aligned} \tag{33}$$

V. GAUGE SECTOR

The gauge sector spectrum arises from the kinetic terms of the scalar bosons, which are given by

$$\mathcal{L} \supset (D_\mu \eta)^\dagger (D^\mu \eta) + (D_\mu \chi)^\dagger (D^\mu \chi) + (D_\mu \sigma)^* (D^\mu \sigma), \quad (34)$$

where the covariant derivative for triplets is defined as

$$D_\mu = \partial_\mu - igW_\mu^a T_a - ig_X X B_\mu - ig_N N N_\mu. \quad (35)$$

Here, $T_a = \frac{\lambda_a}{2}$ are the generators of $SU(3)_L$, with λ_a ($a = 1, \dots, 8$) being the Gell-Mann matrices. The parameters X and N represent the charges of the fields under the $U(1)_X$ and $U(1)_N$ symmetries, respectively. Note that the φ field is a gauge singlet and, therefore, its kinetic term is not included in Eq. (34). The covariant derivative for the σ field only involves the N_μ gauge boson, as σ carries a charge of two under the $U(1)_N$ symmetry.

Since $SU(2)_L \subset SU(3)_L$, the gauge coupling g is the same as in the SM. The gauge bosons associated with the $SU(3)_L$, $U(1)_X$, and $U(1)_N$ symmetries are W_μ^a , B_μ , and N_μ , respectively, with their corresponding gauge couplings denoted as g , g_X , and g_N .

The charged (including the non-Hermitian) gauge bosons are straightforwardly calculated, as they arise from the non-diagonal generators of the $SU(3)_L$ group. The charged gauge eigenstates are given by

$$W_\mu^\pm = \frac{W_{1\mu} \mp iW_{2\mu}}{\sqrt{2}}, \quad V_\mu^{0(\dagger)} = \frac{W_{4\mu} \mp iW_{5\mu}}{\sqrt{2}}, \quad V_\mu^\pm = \frac{W_{6\mu} \pm iW_{7\mu}}{\sqrt{2}}, \quad (36)$$

with masses

$$m_{W^\pm}^2 = \frac{g^2 v_\eta^2}{4}, \quad m_{V^{0(\dagger)}}^2 = \frac{g^2}{4} (v_\eta^2 + v_\chi^2), \quad m_{V^\pm}^2 = \frac{g^2 v_\chi^2}{4}. \quad (37)$$

Note that the fields V_μ^\pm and $V_\mu^{0(\dagger)}$ are P_M -odd, or dark, under the P_M symmetry defined in Eq. (7). However, since the neutral gauge boson is heavier than the charged one, i.e., $m_{V^{0(\dagger)}}^2 = m_{W^\pm}^2 + m_{V^\pm}^2$, the dark gauge sector does not provide a suitable DM candidate.

On the other hand, diagonalization of the squared mass matrix of the neutral gauge bosons is more intricate. In the basis

$$\mathbf{B}_{\text{NG}} = (W_{3\mu}, W_{8\mu}, B_\mu, N_\mu),$$

the mass matrix is given by

$$M_{\text{NG}}^2 = \frac{g^2}{4} \begin{pmatrix} v_\eta^2 & \frac{v_\eta^2}{\sqrt{3}} & -\frac{2g_X v_\eta^2}{3g} & \frac{2g_N v_\eta^2}{3g} \\ \frac{v_\eta^2}{\sqrt{3}} & \frac{v_\eta^2 + 4v_\chi^2}{3} & -\frac{2g_X(v_\eta^2 - 2v_\chi^2)}{3\sqrt{3}g} & \frac{2g_N(v_\eta^2 + 4v_\chi^2)}{3\sqrt{3}g} \\ -\frac{2g_X v_\eta^2}{3g} & -\frac{2g_X(v_\eta^2 - 2v_\chi^2)}{3\sqrt{3}g} & \frac{4g_X^2(v_\eta^2 + v_\chi^2)}{9g^2} & -\frac{4g_N g_X(v_\eta^2 - 2v_\chi^2)}{9g^2} \\ \frac{2g_N v_\eta^2}{3g} & \frac{2g_N(v_\eta^2 + 4v_\chi^2)}{3\sqrt{3}g} & -\frac{4g_N g_X(v_\eta^2 - 2v_\chi^2)}{9g^2} & \frac{4g_X^2(v_\eta^2 + 4(9v_\sigma^2 + v_\chi^2))}{9g^2} \end{pmatrix}. \quad (38)$$

For simplicity, we are neglecting the kinetic mixing term between the Abelian fields B_μ and N_μ .

Since there is a hierarchy between the VEVs, at leading order, the mass matrix M_{NG}^2 is diagonalized by the orthogonal transformation matrix U_{NG} , such that

$$U_{\text{NG}}^T M_{\text{NG}}^2 U_{\text{NG}} = \text{diag}(0, m_Z^2, m_{Z'}^2, m_{Z''}^2),$$

where U_{NG} is approximately

$$U_{\text{NG}} \simeq \begin{pmatrix} \sin \theta_W & \cos \theta_W & -\frac{\sqrt{3}g \tan^2 \theta_W v_\eta^2}{2g_X \tan 2\theta_W v_\chi^2} & \frac{g v_\eta^2}{24g_N v_\sigma^2} \\ -\frac{\sin \theta_W}{\sqrt{3}} & \frac{\sin^2 \theta_W}{\sqrt{3} \cos \theta_W} & -\frac{g \tan \theta_W}{g_X} & \frac{g v_\chi^2}{6\sqrt{3}g_N v_\sigma^2} \\ \frac{g \sin \theta_W}{g_X} & -\frac{g \sin^2 \theta_W}{g_X \cos \theta_W} & -\frac{\tan \theta_W}{\sqrt{3}} & \frac{g_X v_\chi^2}{18g_N v_\sigma^2} \\ 0 & -\frac{g \tan^2 \theta_W v_\eta^2}{24 \cos \theta_W g_N v_\sigma^2} & \frac{g_X v_\chi^2}{6\sqrt{3}g_N \tan \theta_W v_\sigma^2} & 1 \end{pmatrix}. \quad (39)$$

Here, the Weinberg angle θ_W is defined as

$$\sin^2 \theta_W = \frac{g_X^2}{\sqrt{g^2 + \frac{4}{3}g_X^2}}. \quad (40)$$

Since g can be approximately set to 0.652, based on the W^\pm mass, and using $\sin^2 \theta_W \approx 0.231$ [41], the value of g_X is found to be approximately 0.377.

The U_{NG} matrix allows expressing the gauge symmetry bosons, $W_{3\mu}, W_{8\mu}, B_\mu, N_\mu$, in terms of the physical gauge bosons, $A_\mu, Z_\mu, Z'_\mu, Z''_\mu$. That is,

$$\begin{pmatrix} W_{3\mu} \\ W_{8\mu} \\ B_\mu \\ N_\mu \end{pmatrix} = U_{\text{NG}} \begin{pmatrix} A_\mu \\ Z_\mu \\ Z'_\mu \\ Z''_\mu \end{pmatrix}. \quad (41)$$

Besides the fact that the photon mass is zero, we can obtain the masses of the Z , Z' , and Z'' bosons:

$$m_Z^2 \simeq \frac{9g^2 v_\eta^2 v_\chi^2 \cos^2 \theta_W}{\sin^4 \theta_W (v_\eta^2 (36 + v_\chi^2) + 36v_\chi^2) - 36 \sin^2 \theta_W (v_\eta^2 + 2v_\chi^2) + 9 (v_\eta^2 + 4v_\chi^2)}, \quad (42)$$

$$m_{Z'}^2 \simeq \frac{g_X^2 v_\chi^2}{3 \tan^2 \theta_W}, \quad (43)$$

$$m_{Z''}^2 \simeq 4g_N^2 v_\sigma^2. \quad (44)$$

The masses $m_{Z'}$ and $m_{Z''}$ were computed at leading order, while m_Z was computed at the next order, where it deviates from its SM counterpart. However, at leading order, m_Z coincides with the SM Z boson mass, as expected. Additionally, the parameter g_N , together with v_σ , determines the mass of the Z'' , as given in Eq. (44). For v_σ on the order of 10^3 TeV and Yukawa couplings of order 1, the potential remains stable (i.e., $B(\mathbf{n}) > 0$, as defined in Eq. (14)) if $g_N \gtrsim 0.598$.

The Z boson properties in our model deviate from the SM predictions due to the (small) mixing between Z and the other massive vector fields. For example, we can obtain a lower bound on v_χ by imposing that the new contribution to the ρ_0 parameter, defined as $\rho_0 \equiv \left(\frac{M_W}{M_Z \cos \theta_W} \right)^2$, remain within the experimental limits [42]. This parameter, which is exactly equal to unity in the SM, is modified in our model as:

$$\Delta\rho_0 = \rho_0 - 1 \approx \frac{v_\eta^2 \cos^2 2\theta_W \sec^4 \theta_W}{4v_\chi^2}. \quad (45)$$

Using $\sin^2 \theta_W \approx 0.231$ and the allowed experimental deviation $\Delta\rho_0 \lesssim 5.8 \times 10^{-4}$ [42], we find that

$$v_\chi \gtrsim 3571.35 \text{ GeV}, \quad (46)$$

setting the lower bound for the symmetry breaking scale of the 331 model.

VI. YUKAWA SECTOR: SEESAW-SUPPRESSED FERMION MASSES

In this section, we derive the fermion mass spectrum, demonstrating how seesaw mechanisms emerge across all sectors as a result of the VEV hierarchy $v_\eta \ll v_\chi \ll v_\varphi, v_\sigma$. The electroweak VEV, v_η , is fixed at $v_{\text{SM}} = 246$ GeV, while the 3-3-1 breaking VEV, v_χ , is significantly larger, approximately 3.6 TeV. An even larger VEV, v_φ , is required to enable the seesaw mechanism for charged fermions, with v_φ typically around 10^6 GeV. Finally, the $B - L$ symmetry-breaking VEV, v_σ , must also be large, satisfying $v_\sigma \gg v_\eta$, to justify the seesaw mechanism for neutrinos. This hierarchical structure plays a crucial role in shaping the Yukawa sector.

These seesaw mechanisms not only provide a partial explanation for the flavor puzzle but also help identify the fermionic dark matter candidate in our model. By incorporating this hierarchy, the model successfully reproduces the observed fermion mass spectrum and offers a natural framework to address open questions in particle physics, such as the flavor puzzle and the nature of dark matter.

A. Lepton Spectrum

The renormalizable Yukawa Lagrangian for the lepton sector is expressed as:

$$\begin{aligned}
-\mathcal{L}_l = & Y_{ij}^\nu \overline{L_{iL}} \eta \nu_{jR} + Y_{ij}^f \overline{L_{iL}} \chi f_{jR} + \frac{h_{ij}^\nu}{2} \sigma (\nu_{iR})^c \nu_{jR} + \frac{h_{ij}^f}{2} \varphi (f_{iR})^c f_{jR} \\
& + y_{ij}^{\mathcal{F}} \overline{L_{iL}} \eta^* \mathcal{F}_{jR} + y_{ij}^e \overline{\mathcal{F}_{iL}} \chi^* e_{jR} + h_{ij}^{\mathcal{F}} \varphi \overline{\mathcal{F}_{iL}} \mathcal{F}_{jR} + \text{h.c.}
\end{aligned} \tag{47}$$

Following spontaneous symmetry breaking, all leptons acquire mass, as will be demonstrated in the subsequent analysis. It is also noteworthy that all Yukawa couplings in the lepton sector are represented by 3×3 matrices. For simplicity, we omit explicit indices and work directly with the couplings in matrix form. Furthermore, we assume that all Yukawa parameters are real, as CP violation is not considered in this analysis.

1. Charged Leptons

The charged lepton sector consists of P_M -even fields (e_i and E_i^l), which mix to produce the SM charged leptons and three heavy charged leptons, as well as P_M -odd fields (E_i), where $i = 1, 2, 3$.

In the basis $\mathbf{E}_{L,R} = (e_{L,R}, E_{L,R}^l)$, the mass terms are expressed as $\overline{\mathbf{E}}_L \mathcal{M}_e \mathbf{E}_R$, where the mass matrix \mathcal{M}_e is given by:

$$\mathcal{M}_e = \begin{pmatrix} 0 & -y^{\mathcal{F}} v_\eta \\ y^e v_\chi & h^{\mathcal{F}} v_\varphi \end{pmatrix}. \tag{48}$$

This mass matrix exhibits a type-I Dirac seesaw structure in the limit $v_\eta \ll v_\chi \ll v_\varphi$. To leading order, the matrix \mathcal{M}_e can be block-diagonalized using two unitary matrices, V_L^e and V_R^e . The diagonalization matrices are given by:

$$V_L^e = \begin{pmatrix} 1 & -\frac{v_\eta}{v_\varphi} y^{\mathcal{F}} (h^{\mathcal{F}})^{-1} \\ \frac{v_\eta}{v_\varphi} (h^{\mathcal{F}\dagger})^{-1} y^{\mathcal{F}\dagger} & 1 \end{pmatrix}, \quad V_R^e = \begin{pmatrix} 1 & \frac{v_\chi}{v_\varphi} y^{e\dagger} (h^{\mathcal{F}\dagger})^{-1} \\ \frac{v_\chi}{v_\varphi} (h^{\mathcal{F}})^{-1} y^e & 1 \end{pmatrix}, \tag{49}$$

such that

$$V_L^{e\dagger} \mathcal{M}_e V_R^e = \text{diag}(M_e, M_{E'}), \quad (50)$$

where the mass matrices are given by

$$M_e = \frac{v_\eta v_\chi}{\sqrt{2} v_\varphi} y^{\mathcal{F}} (h^{\mathcal{F}})^{-1} y^e, \quad M_{E'} = \frac{v_\varphi}{\sqrt{2}} h^{\mathcal{F}}. \quad (51)$$

The mass matrix of P_M -odd fields, E_i , is

$$M_E = \frac{v_\varphi}{\sqrt{2}} h^{\mathcal{F}}, \quad (52)$$

that is they are essentially degenerate with P_M -even fields E'_i .

For simplicity, we assume $y^{\mathcal{F}} = h^{\mathcal{F}}$ equal to the identity matrix and y^e to be diagonal. This allows us to express the matrix elements in terms of the masses of the charged leptons e , μ , and τ . The diagonal Yukawa coupling matrix is then given by:

$$y^e = \text{diag}(y_1^e, y_2^e, y_3^e). \quad (53)$$

By solving for the matrix elements, we find the following relations:

$$y_1^e = \frac{\sqrt{2} v_\varphi}{v_\eta v_\chi} m_e, \quad y_2^e = \frac{\sqrt{2} v_\varphi}{v_\eta v_\chi} m_\mu, \quad y_3^e = \frac{\sqrt{2} v_\varphi}{v_\eta v_\chi} m_\tau. \quad (54)$$

Considering the masses given in [42], with $v_\eta = v_{\text{SM}}$, $v_\chi = 5 \cdot 10^3$ GeV, and $v_\varphi = 10^6$ GeV, the Yukawa parameters y^e are of the orders:

$$y_3^e \sim 1, \quad y_2^e \sim 10^{-2}, \quad y_1^e \sim 10^{-4}. \quad (55)$$

2. Neutrinos

The neutral lepton spectrum can be divided into the P_M -even (visible) and P_M -odd (dark) sectors. The P_M -even sector corresponds to neutrinos. We define the basis $\mathbf{N}_L = (\nu_L, (\nu_R)^c)$ and write the mass term as $(1/2) \overline{\mathbf{N}}_L \mathcal{M}_\nu (\mathbf{N}_L)^c$, where the mass matrix \mathcal{M}_ν is given by:

$$\mathcal{M}_\nu = \frac{1}{\sqrt{2}} \begin{pmatrix} 0 & Y^\nu v_\eta \\ Y^{\nu T} v_\eta & h^\nu v_\sigma \end{pmatrix}. \quad (56)$$

Since $v_\sigma \gg v_\eta$, the matrix \mathcal{M}_ν exhibits the structure of a type-I seesaw mechanism [43]. To leading order, it can be block-diagonalized by the matrix V^ν , given by:

$$V^\nu = \begin{pmatrix} 1 & \frac{v_\eta}{v_\sigma} Y^{\nu*} (h^{\nu*})^{-1} \\ -\frac{v_\eta}{v_\sigma} (h^{\nu T})^{-1} Y^{\nu T} & 1 \end{pmatrix}, \quad (57)$$

such that

$$V^{\nu T} \mathcal{M}_\nu V^\nu = \text{diag}(m_\nu, m_N), \quad (58)$$

where the mass matrices are:

$$m_\nu = -\frac{v_\eta^2}{\sqrt{2}v_\sigma} Y^\nu (h^\nu)^{-1} Y^{\nu T}, \quad m_N = \frac{v_\sigma}{\sqrt{2}} h^\nu. \quad (59)$$

For simplicity, we assume h^ν to be diagonal, as sterile neutrino oscillations are not considered in this work. Using the Casas-Ibarra parameterization ([44], [45]), and considering the R matrix as the identity matrix, we obtain the solution for Y^ν

$$Y^\nu = -i \frac{\sqrt{\sqrt{2}v_\sigma}}{v_\eta} (m_\nu^{\text{diag}})^{1/2} U_{2\nu}^{-1} = -i \frac{\sqrt{\sqrt{2}v_\sigma}}{v_\eta} (m_\nu^{\text{diag}})^{1/2} (U_{\text{PMNS}}^{-1})^\dagger. \quad (60)$$

In the last equality, we use $U_{2\nu} = U_{\text{PMNS}}^\dagger$ [46], as the charged lepton mass matrix is diagonal under our assumptions. Hence, this result expresses the elements of the Yukawa matrix Y^ν in terms of the neutrino masses $m_{\nu i}$ (for $i = 1, 2, 3$), which correspond to the physical neutrinos ν_{iL} , and the neutrino mixing angles in U_{PMNS} .

3. Dark Leptons

The P_M -odd, or dark, neutral leptons are arranged in the basis $\mathbf{F}_L = (f_L, (f_R)^c, (f'_L), (f'_R)^c)$, such that their mass matrix, $(1/2) \overline{\mathbf{F}}_L \mathcal{M}_f (\mathbf{F}_L)^c$, is expressed as

$$\mathcal{M}_f = \begin{pmatrix} 0_{[3 \times 3]} & m_D^f_{[3 \times 9]} \\ (m_D^f)^T_{[9 \times 3]} & m_R^f_{[9 \times 9]} \end{pmatrix}, \quad (61)$$

where

$$m_D^f = \frac{1}{\sqrt{2}} \begin{pmatrix} Y^f v_\chi & 0 & 0 \\ 0 & -y^{\mathcal{F}} v_\eta \end{pmatrix}, \quad m_R^f = \frac{1}{\sqrt{2}} \begin{pmatrix} h^f v_\varphi & 0 & 0 \\ 0 & h^{\mathcal{F}} v_\varphi & 0 \\ 0 & 0 & h^{\mathcal{F}T} v_\varphi \end{pmatrix}. \quad (62)$$

The structure corresponds to a type-I seesaw, as the eigenvalues of m_R^f are proportional to v_φ , while the entries of m_D^f are at most proportional to v_χ , with $v_\varphi \gg v_\chi \gg v_\eta$. Therefore, the same procedure applied to neutrinos can be repeated. In this case, however, block diagonalization requires two matrices, V_1^f and V_2^f . The transformation is given by

$$V_2^{fT} V_1^{fT} \mathcal{M}_f V_1^f V_2^f = \text{diag}(m_f, m_{f'_1}, m_{f'_2}, m_{f'_3}),$$

where the block matrices on the diagonal are

$$m_f = -\frac{v_\chi^2}{\sqrt{2}v_\varphi} Y^f (h^{\mathcal{F}})^{-1} Y^{fT}, \quad m_{f'_1} = \frac{v_\varphi}{\sqrt{2}} h^f, \quad m_{f'_2} = \frac{v_\varphi}{\sqrt{2}} h^{\mathcal{F}}, \quad m_{f'_3} = -\frac{v_\varphi}{\sqrt{2}} h^{\mathcal{F}}. \quad (63)$$

The matrices V_1^f and V_2^f are explicitly given by:

$$V_1^f = \begin{pmatrix} 1 & \frac{v_\chi}{v_\varphi} Y^{f*} (h^{f*})^{-1} & -\frac{v_\eta}{v_\varphi} y^{\mathcal{F}*} (h^{\mathcal{F}*})^{-1} & 0 \\ -\frac{v_\chi}{v_\varphi} (h^{fT})^{-1} Y^{fT} & 1 & 0 & 0 \\ -\frac{v_\eta}{v_\varphi} (h^{\mathcal{F}T})^{-1} y^{\mathcal{F}T} & 0 & 1 & 0 \\ 0 & 0 & 0 & 1 \end{pmatrix}, \quad V_2^f = \begin{pmatrix} 1 & 0 & 0 & 0 \\ 0 & 1 & 0 & 0 \\ 0 & 0 & \frac{1}{\sqrt{2}} & -\frac{1}{\sqrt{2}} \\ 0 & 0 & \frac{1}{\sqrt{2}} & \frac{1}{\sqrt{2}} \end{pmatrix}. \quad (64)$$

As a result, three of the dark neutral leptons acquire seesaw-suppressed masses originating from the m_f matrix and are significantly lighter than the others. The lightest of these fermions serves as the DM candidate.

B. Quark Spectrum

We now proceed to apply a similar analysis to the quark sector, detailing the corresponding Yukawa interactions. The general Yukawa Lagrangian for the quarks is written as:

$$\begin{aligned} -\mathcal{L}_q &= Y_{aj}^d \overline{Q_{aL}} \eta^* d_{jR} + Y_{ab}^D \overline{Q_{aL}} \chi^* D_{bR} + Y_{3j}^U \overline{Q_{3L}} \eta u_{jR} + Y_{33}^U \overline{Q_{3L}} \chi U_{3R} \\ &+ y_{ab}^\mathcal{K} \overline{Q_{aL}} \eta \mathcal{K}_{bR} + y_{33}^\mathcal{K} \overline{Q_{3L}} \eta^* \mathcal{K}_{3R} + y_{aj}^u \overline{\mathcal{K}_{aL}} \chi u_{jR} + y_{3i}^d \overline{\mathcal{K}_{3L}} \chi^* d_{iR} \\ &+ h_{ab}^\mathcal{K} \varphi \overline{\mathcal{K}_{aL}} \mathcal{K}_{bR} + h_{33}^\mathcal{K} \varphi \overline{\mathcal{K}_{3L}} \mathcal{K}_{3R} + \text{h.c.}, \end{aligned} \quad (65)$$

where $a, b = 1, 2$ and $i, j = 1, 2, 3$.

1. *Up-type Quarks*

Starting with the P_M -even up-type quarks, we obtain the following mass matrix when written in the basis $\mathbf{u} = (u_i, \mathcal{U}'_a)$:

$$\mathcal{M}_u = \frac{1}{\sqrt{2}} \begin{pmatrix} 0_{[2 \times 3]} & y_{[2 \times 2]}^{\mathcal{K}} v_\eta \\ Y_{[1 \times 3]}^u v_\eta & 0_{[1 \times 2]} \\ y_{[2 \times 3]}^u v_\chi & h_{[2 \times 2]}^{\mathcal{K}} v_\varphi \end{pmatrix}. \quad (66)$$

For the sake of clarity, since the quark Yukawa couplings have different dimensions, we explicitly write their dimensions in the mass matrices throughout this section.

The hierarchy between the blocks allows us to employ the seesaw approximation used in the previous section. We do not provide all the details here, as the procedure is quite similar to the one applied in the lepton sector. After performing the block-diagonalization, we obtain the following two matrices:

$$(m_u^2)_{\text{light}} \simeq \frac{v_\eta^2}{2} \begin{pmatrix} \kappa_\chi^2 A [1 - Y^{u\dagger} (Y^u Y^{u\dagger})^{-1} Y^u] A^\dagger & 0_{[2 \times 1]} \\ 0_{[1 \times 2]} & Y^u Y^{u\dagger} \end{pmatrix}, \quad (67)$$

and

$$(M_u^2)_{\text{heavy}} \simeq \frac{v_\varphi^2}{2} h^{\mathcal{K}} h^{\mathcal{K}\dagger}, \quad (68)$$

where $A_{[2 \times 3]} = y^{\mathcal{K}} h^{\mathcal{K}-1} y^u$ and $\kappa_\chi = v_\chi/v_\varphi$.

Consequently, two of the three light up-type quarks acquire seesaw-suppressed masses, proportional to $v_\eta \kappa_\chi$. Meanwhile, the remaining quark has a mass proportional to the electroweak scale, v_η , and is identified as the top quark.

We can determine a constraint on the Y^u matrix related to the top quark. According to [41], the top quark mass is 172.57 ± 0.29 GeV. Thus, we have:

$$\sqrt{\frac{v_\eta^2}{2} Y^u (Y^u)^\dagger} = \frac{v_\eta}{\sqrt{2}} \sqrt{Y_1^{u2} + Y_2^{u2} + Y_3^{u2}} \sim 172.57, \quad (69)$$

from which we obtain:

$$Y_t \equiv \sqrt{Y_1^{u2} + Y_2^{u2} + Y_3^{u2}} \sim 1. \quad (70)$$

The Yukawa coupling is constrained to be less than 1.67 at 95% confidence level (C.L.) [47].

Regarding the P_M -odd up-quarks, we choose $\mathbf{U} = (U_3, \mathcal{U}_3, \mathcal{U}_a)$ as the basis. In this framework, the mass matrix for the dark up-type quarks is given by:

$$\mathcal{M}_u^{\text{dark}} = \frac{1}{\sqrt{2}} \begin{pmatrix} Y_{33}^U v_\chi & -y_{33}^\mathcal{K} v_\eta & 0_{[1 \times 2]} \\ 0 & h_{33}^\mathcal{K} v_\varphi & 0_{[1 \times 2]} \\ 0_{[2 \times 1]} & 0_{[2 \times 1]} & h_{[2 \times 2]}^\mathcal{K} v_\varphi \end{pmatrix}. \quad (71)$$

It is clear that \mathcal{U}_a does not mix with the other quarks, and their mass matrix corresponds to the bottom-right block of $\mathcal{M}_u^{\text{dark}}$. For the remaining two states, there is a small mixing of order $\mathcal{O}(v_\eta/v_\varphi)$, and their masses are approximately given by the upper diagonal entries of $\mathcal{M}_u^{\text{dark}}$.

2. Down-type Quarks

For the P_M -even down-type quarks, we choose $\mathbf{d} = (d_i, \mathcal{D}'_3)$ as the basis and derive the mass matrix as follows:

$$\mathcal{M}_d = \frac{1}{\sqrt{2}} \begin{pmatrix} Y_{[2 \times 3]}^d v_\eta & 0_{[2 \times 1]} \\ 0_{[1 \times 3]} & -y_{33}^\mathcal{K} v_\eta \\ y_{[1 \times 3]}^d v_\chi & h_{33}^\mathcal{K} v_\varphi \end{pmatrix}. \quad (72)$$

Following the seesaw procedure, the diagonalization of $\mathcal{M}_d \mathcal{M}_d^\dagger$ proceeds analogously to the lepton case. The masses are approximately given by:

$$(m_d^2)_{\text{light}} \simeq \frac{v_\eta^2}{2} \begin{pmatrix} Y^d Y^{d\dagger} & 0_{[2 \times 1]} \\ 0_{[1 \times 2]} & \kappa_\chi^2 B [1 - Y^{d\dagger} (Y^d Y^{d\dagger})^{-1} Y^d] B^\dagger \end{pmatrix}, \quad (73)$$

$$(M_d^2)_{\text{heavy}} \simeq \frac{v_\varphi^2}{2} |h_{33}^\mathcal{K}|^2. \quad (74)$$

where $B_{[1 \times 3]} = \frac{y_{33}^\mathcal{K}}{h_{33}^\mathcal{K}} y^d$. As a result, among the down-type quarks, only one acquires a seesaw-suppressed mass.

Finally, we considered the P_M -odd down-quarks. To analyze this, we fix the basis for the dark down-type quarks as $\mathbf{D} = (D_a, \mathcal{D}_a, \mathcal{D}_3)$. The resulting mass matrix is given by:

$$\mathcal{M}_d^{\text{dark}} = \frac{1}{\sqrt{2}} \begin{pmatrix} Y_{[2 \times 2]}^D v_\chi & y_{[2 \times 2]}^\mathcal{K} v_\eta & 0_{[2 \times 1]} \\ 0_{[2 \times 2]} & h_{[2 \times 2]}^\mathcal{K} v_\varphi & 0_{[2 \times 1]} \\ 0_{[1 \times 2]} & 0_{[1 \times 2]} & h_{33}^\mathcal{K} v_\varphi \end{pmatrix}. \quad (75)$$

The diagonal entries provide the approximate masses. While \mathcal{D}_3 remains unmixed, the fields D_a and \mathcal{D}_a exhibit a small mixing suppressed by $\kappa_\eta = v_\eta/v_\varphi$.

In summary, this section demonstrated that all fermions acquire mass through a consistent application of the seesaw mechanism, highlighting its universality across the entire fermion sector.

VII. BOUNDS FROM CHARGED LEPTONS

The flavor-violating Yukawa couplings are obtained from Eq. (47). After the block-diagonalization, keeping the leading order, the charged lepton Yukawa couplings can be divided into pure SM lepton couplings

$$\mathcal{L}_{\text{SM}} = \frac{\sqrt{2}}{v_\eta} \bar{e}_L M_e e_R \eta_1^{0*} + \frac{\sqrt{2}}{v_\chi} \bar{e}_L M_e e_R \chi_3^{0*} - \frac{\sqrt{2}}{v_\varphi} \bar{e}_L M_e e_R \varphi + \text{h.c.}, \quad (76)$$

and couplings containing exotic charged leptons

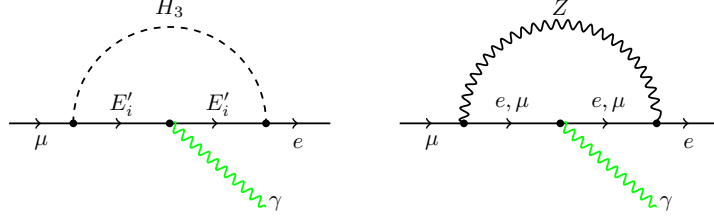
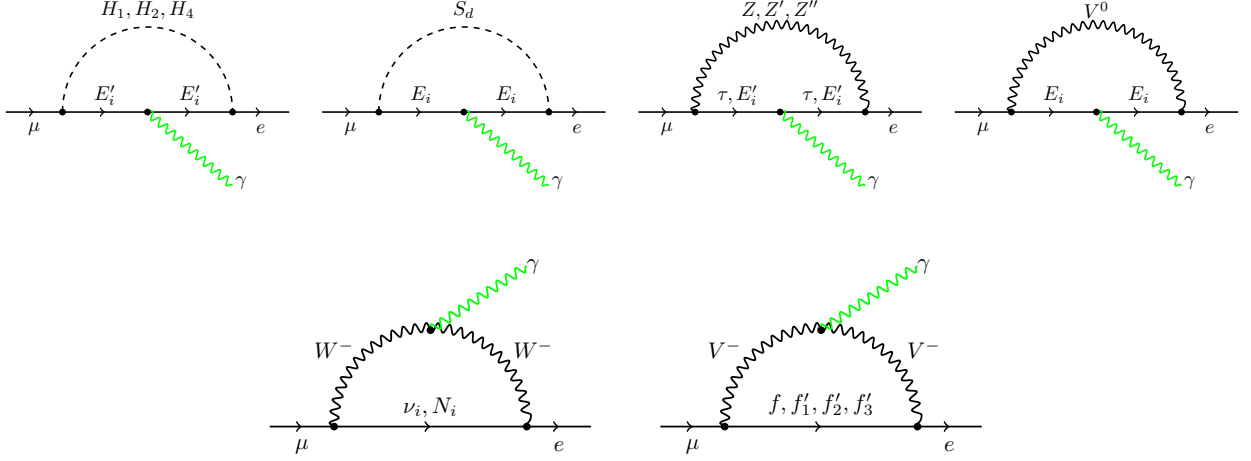
$$\mathcal{L}_{\text{exotic}} = -\bar{e}_L y^F E'_R \eta_1^{0*} + \bar{e}_L y^F E_R \eta_3^{0*} + \bar{E}_L y^e e_R \chi_1^{0*} + \bar{E}'_L y^e e_R \chi_3^{0*} + \bar{E}_L h^F E_R \varphi + \bar{E}'_L h^F E'_R \varphi + \text{h.c.} \quad (77)$$

The charged lepton mass matrices in Eqs. (52) and (51) are diagonalized in the form $U_L^{l\dagger} M_l U_R^l = M_l^{\text{diag}}$ and physical coupling constants in Eq. (77) become

$$y^{\mathcal{F}} \rightarrow \tilde{y}^{\mathcal{F}} = U_L^{e\dagger} y^{\mathcal{F}} U_R^E, \quad y^e \rightarrow \tilde{y}^e = U_L^{E\dagger} y^e U_R^e, \quad h^{\mathcal{F}} \rightarrow \tilde{h}^{\mathcal{F}} = U_L^{E\dagger} h^{\mathcal{F}} U_R^E. \quad (78)$$

One can see that the Yukawa couplings of SM charged-leptons are proportional to their mass matrix and are therefore diagonalized simultaneously with the SM lepton mass matrix. Therefore the neutral scalars do not have flavor-changing neutral currents at the tree level. This also avoids the LHC bounds on the lepton flavor-violating couplings of Higgs. The SM lepton couplings are all suppressed by heavy VEVs, except the first one in Eq. (76). The muon and tau Yukawa couplings have been measured at LHC to be close to the SM values. Therefore the real part of η_1^0 needs to be identified with 125 GeV Higgs. The lepton masses are suppressed by v_χ/v_φ . This imposes $v_\chi/v_\varphi \gtrsim 10^{-2}$, in order to keep Yukawa coupling smaller than 1.

Even though scalars do not have flavor-changing couplings to a pair of SM charged leptons, the flavor-violating effects appear at the loop level due to the mixing between SM leptons and the charged exotic leptons. The most constraining charged lepton flavor-violating (CLFV) process is $\mu \rightarrow e\gamma$, where all neutral scalars and massive gauge bosons mediate it at loop level. The most constraining CLFV diagrams

FIG. 1. The dominant diagrams contributing to $\mu \rightarrow e\gamma$.FIG. 2. Sub-leading diagrams contributing to $\mu \rightarrow e\gamma$.

are presented in Fig. 1 and sub-leading diagrams in Fig. 2. Note that the photon vertex is always flavor conserving. The couplings between scalars, SM charged leptons and E'_i are not suppressed by the mixing between SM leptons and exotic leptons, as can be seen in Eq. (77). The scalar mediated diagrams are, however, heavily suppressed by large masses of E'_i and E_i , as well as the relation

$$\tilde{y}^F (M_{E'}^{\text{diag}})^{-1} \tilde{y}^e = \frac{2}{v_\eta v_\chi} M_e^{\text{diag}}, \quad (79)$$

which originates from the seesaw mechanism. The leading contribution to the scalar diagrams is canceled due to this relation, providing further suppression. The most relevant scalar diagram is mediated by H_3 , corresponding to the branching ratio

$$\text{BR}(\mu \rightarrow e\gamma) = \frac{e^2 \alpha_{13}^2 \alpha_{23}^2 m_\mu^3 m_{H_3}^4}{64 (4\pi)^5 \Gamma_\mu^{\text{tot}}} \left(\left| \sum_{i=1}^3 \frac{\tilde{y}_{ie}^e \tilde{y}_{\mu i}^F}{m_{E'_i}^3} \right|^2 + \left| \sum_{i=1}^3 \frac{\tilde{y}_{i\mu}^e \tilde{y}_{ei}^F}{m_{E'_i}^3} \right|^2 \right), \quad (80)$$

where Γ_μ^{tot} is the total muon decay width. We can obtain a conservative bound by setting the $m_{H_3}, m_{E'_i} \sim$

v_φ and the flavor-violating couplings to unity:

$$\left(\frac{\text{GeV}}{v_\varphi}\right) \alpha_{13}\alpha_{23} < 1.55 \times 10^{-10}, \quad (81)$$

which is satisfied for $v_\varphi > 10^6 \text{GeV}$ and $\alpha_{13}, \alpha_{23} < 10^{-2}$. So even with large, $\mathcal{O}(1)$, flavor-violating couplings, bound from this diagram can be avoided.

The diagrams mediated by the exotic gauge bosons are suppressed by their heavy masses. The couplings involved are also tiny, $\sim v_\eta/v_\varphi$, due to them being a result of mixing between SM leptons and exotic ones. These diagrams provide an insignificant contribution to $\mu \rightarrow e\gamma$. The diagrams mediated by W boson are suppressed due to tiny ν_i masses or small mixing between heavy and light neutrinos. The only relevant diagram mediated by gauge bosons is the Z boson mediated one in Figure 1. It is suppressed only by one flavor-violating coupling and is not mass suppressed due to Z boson being relatively light. It provides contribution comparable to H_3 mediated diagram. The $\mu \rightarrow e\gamma$ branching ratio corresponding to Z boson mediated diagram is,

$$\text{BR}(\mu \rightarrow e\gamma) = \frac{e^2 g^4 m_\mu^5 v_\chi^4 \sin^2 \theta_W \tan^2 \theta_W}{144(4\pi)^5 \Gamma_\mu^{\text{tot}} m_z^4} \left| \frac{3g_3^2}{g_x^2} \Lambda_{\mu e}^* + 3\Lambda_{e\mu} \right|^2, \quad (82)$$

where

$$\Lambda = \tilde{y}^{e\dagger} ((m_{E'}^{\text{diag}})^{-1})^2 \tilde{y}^e. \quad (83)$$

We can obtain a conservative bound by setting $\Lambda \sim 1/v_\varphi^2$

$$\frac{v_\chi}{v_\varphi} < 7.7 \times 10^{-3}. \quad (84)$$

In conclusion the CLFV constraints are easily avoided, even with large flavor-violating couplings. As mentioned in Section VIA 1, in our numerics for the dark matter phenomenology we made the simplifying assumptions of making the Yukawa couplings diagonal. In that case the CLFV effects are absent.

VIII. DARK MATTER

As previously mentioned, after the symmetry breaking of the 3-3-1-1 gauge symmetry, the P_M symmetry naturally emerges within the model. This discrete symmetry plays a crucial role in stabilizing the lightest P_M -odd particle, which, being electrically neutral, serves as a compelling DM candidate. This particle could account for the DM relic abundance measured by the Planck satellite [48], given by:

$$\Omega_{\text{DM}} h^2 = 0.1200 \pm 0.0012.$$

The model predicts the existence of neutral P_M -odd particles across all sectors: scalar, fermion, and gauge. Specifically, these include the scalar S_d in Eq. (26), the gauge boson V^0 in Eq. (36), and the leptons, which are the eigenstates of the mass matrices defined in Eq. (63). However, as P_M is a Z_2 discrete symmetry, the model does not support a multi-component DM sector.

The V^0 gauge boson is not a suitable DM candidate because its mass, given by $m_{V^0(\mp)}^2 = m_{W^\pm}^2 + m_{V^\pm}^2$, allows it to decay into W^\pm and V^\mp . Since V^\pm is also a P_M -odd particle, this decay renders V^0 unstable, disqualifying it as a viable DM candidate. As for the scalar candidate, S_d , while it could theoretically provide the correct relic density, it is completely ruled out by current experimental constraints on the spin-independent direct detection cross-section, which exclude all regions of its parameter space. Consequently, we will not consider it further in this work.

On the other hand, the dark fermion sector offers a promising candidate for DM. Specifically, the lightest eigenstate of the mass matrix m_f in Eq. (63), which we denote as f_d , emerges as a viable DM candidate. The remaining dark leptons, i.e., the eigenstates of $m_{f'_1}$, $m_{f'_2}$, and $m_{f'_3}$, are extremely heavy, with masses proportional to $v_\varphi \sim 10^6$ GeV. Consequently, they do not contribute to the DM phenomenology and are integrated out in the effective Lagrangian.

In fact, not only are the heavy dark leptons integrated out, but all particles with masses on the order of v_σ and v_φ are as well, as they do not play a significant role in the DM analysis. This is because the focus is on DM candidates with masses in the range of 10 GeV to 1.5 TeV, a range that aligns with the sensitivity of current and upcoming accelerator experiments.

To analyze the phenomenology of DM, we begin by fixing certain parameters of the model. We first focus on the lepton Lagrangian, where the relevant parameters are Y^ν , Y^f , h^ν , h^f , $y^{\mathcal{F}}$, y^e , and $h^{\mathcal{F}}$. All these quantities are 3×3 matrices.

The matrices $h^{\mathcal{F}}$, h^ν , and h^f are required to be of order one to preserve the validity of the see-saw mechanism in both the charged and neutral lepton sectors. For simplicity, we assume h^ν and h^f matrices to be equal to the identity matrix and $h^{\mathcal{F}}$ to be 0.5 times the identity matrix. Similarly, the $y^{\mathcal{F}}$ matrix is also taken as the identity matrix. The y^e matrix, in contrast, is diagonal, with its elements specified by Eq. (54), ensuring compatibility with the SM charged leptons. The Y^ν matrix is derived using Eq. (60) to reproduce the active neutrino masses and mixings, consistent with neutrino oscillation data [46].

Finally, the Yukawa coupling matrix Y^f , assumed to be diagonal for simplicity, is constrained by $Y^f < \sqrt{4\pi} \mathbb{1}$ to maintain the perturbative regime. The diagonal elements of this matrix are directly linked to the masses of the dark leptons, m_f , as specified in Eq. (63).

In a similar manner, we fixed the parameters in the quark sector, which include the matrices Y_{aj}^d , Y_{ab}^D , Y_{3j}^u , Y_{33}^U , $y_{ab}^{\mathcal{K}}$, $y_{33}^{\mathcal{K}}$, y_{aj}^u , y_{3i}^d , $h_{ab}^{\mathcal{K}}$, and $h_{33}^{\mathcal{K}}$, where $a, b = 1, 2$ and $i, j = 1, 2, 3$. Among these, Y^d and Y^u are determined to reproduce the SM quark masses. For simplicity, the remaining matrices are chosen to be equal to the identity. This assumption is consistent with the seesaw mechanism, which is also present in the quark sector. It is important to emphasize that exotic quarks, with masses on the order of v_χ , do not significantly influence the DM analysis. At this point, we have fixed the parameter space in the scalar sector. Equation (16) enables all quartic couplings to be expressed in terms of the scalar masses and rotation angles, as defined in Eq. (18). Additionally, three of these angles have been reformulated in terms of the VEVs, as shown in Eq. (20). Based on the previous discussion, the free parameters used in our DM analysis are: α_{12} , α_{13} , α_{23} , m_{H_2} , m_{H_3} , v_χ , v_σ , and v_φ . Specifically, the ranges and relationships are defined as follows. For the mixing angles, the allowed intervals are:

$$10^{-3} \leq |\alpha_{12}| \leq 0.32, \quad 10^{-4} \leq |\alpha_{13}| \leq 10^{-3}, \quad 10^{-4} \leq |\alpha_{23}| \leq 10^{-2}. \quad (85)$$

The angles, in radians, are chosen such that all quartic couplings satisfy the perturbative unitarity constraints discussed in Sec. IV. The vacuum expectation values are constrained by:

$$3.6 \text{ TeV} \leq v_\chi \leq 12 \text{ TeV}, \quad 10^2 \text{ TeV} \leq v_\sigma \leq 1.5 \cdot 10^3 \text{ TeV}, \quad 10^3 \text{ TeV} \leq v_\varphi \leq 2.5 \cdot 10^3 \text{ TeV}. \quad (86)$$

Finally, the masses of the scalar particles are given by:

$$1 \text{ TeV} \leq m_{H_2} \leq 10 \text{ TeV}, \quad 2 \text{ TeV} \leq m_{H_3} \leq 10 \text{ TeV}. \quad (87)$$

With all parameters established, we now proceed to calculate the DM relic density, $\Omega_{\text{DM}} h^2$, resulting from the freeze-out of f_d . To achieve this, we follow the standard procedures outlined in Refs. [49, 50]. These procedures involve solving the Boltzmann equation for the DM yield Y , defined as $Y \equiv n/s$ (the ratio of number density to entropy density), which is expressed as:

$$\frac{dY}{dx} = - \left(\frac{45}{\pi} G \right)^{-1/2} \frac{g_*^{1/2} m_{f_d}}{x^2} \langle \sigma v \rangle_{\text{ann}} (Y^2 - Y_{\text{eq}}^2). \quad (88)$$

Here, $x = m_{f_d}/T$ represents the dimensionless temperature variable, G denotes the gravitational constant, and $Y_{\text{eq}} = n_{\text{eq}}/s$ is the equilibrium yield. The equilibrium number density, n_{eq} , and the effective number of relativistic degrees of freedom, g_* , are defined following the formalism outlined in Ref. [49]. Finally, $\langle \sigma v \rangle_{\text{ann}}$ corresponds to the thermally averaged annihilation cross section, a key quantity in the freeze-out

calculation. Once the Boltzmann equation is solved and the DM yield Y is determined at the present time (Y_0), the relic density is computed as:

$$\Omega_{\text{DM}} h^2 = 2.82 \times 10^8 \times Y_0 \times \frac{m_{f_d}}{\text{GeV}}. \quad (89)$$

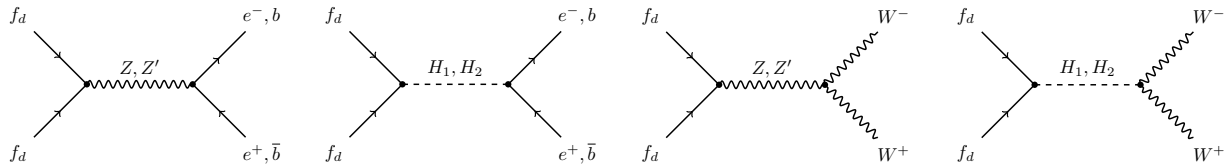


FIG. 3. Main processes contributing to the annihilation of the DM fermion f_d into SM particles.

Due to the complexity of the model and the extensive parameter space defined in Eqs. (85)–(87), solving the Boltzmann equation (88) presents a significant computational challenge. This difficulty arises primarily from the calculation of $\langle\sigma v\rangle_{\text{ann}}$, which, in our case, is dominated by the annihilation processes depicted in Fig. 3. To address this, we employ the packages `Feynrules` [51, 52], `CalcChep` [53], and `MicrOMEGAs` [54], which are widely used tools in phenomenological studies of dark matter. Specifically, we used the `MicrOMEGAs` package to scan over the DM mass in the range $10 \text{ GeV} \leq m_{f_d} \leq 1500 \text{ GeV}$ and varied the remaining parameters within the ranges defined in Eqs. (85)–(87). Our results are presented in Fig. 4. The horizontal band in this figure represents the measured relic density, $\Omega_{\text{DM}} h^2$, at the 3σ level, as reported by the Planck collaboration [48]. It is evident that the fermionic dark matter candidate in this model satisfies the relic density constraint within the range $160 \text{ GeV} \lesssim m_{f_d} \lesssim 520 \text{ GeV}$ and also around the Higgs resonance $\sim 62.5 \text{ GeV}$.

To better understand this range and identify key parameters that ensure the model’s consistency with the relic density, we have also considered specific scenarios. In addition to the green region, which represents a logarithmic random scan over the parameters in Eqs. (85)–(87), we have identified six benchmark scenarios, depicted by the colored lines. In these scenarios, the parameters α_{13} , α_{23} , and m_{S_d} are fixed at 0.003, 0.03, and 5 TeV, respectively. For $v_\chi = 3.6 \text{ TeV}$, $m_{H_2} = 1 \text{ TeV}$ and $v_\chi = 8 \text{ TeV}$, $m_{H_2} = 2.5 \text{ TeV}$, the angle α_{12} , measured in radians, was taken to be 0.06, 0.10, or 0.32, as this parameter plays a critical role in enabling the efficient annihilation of f_d into SM particles, such as the Higgs bosons, as well as into $H_{2,3}$ and Z' , which are associated with the 3-3-1 energy scale. Specifically, Fig. 4 illustrates that as α_{12} increases, the Higgs resonance effects become more pronounced. The relic density observed by the Planck collaboration is obtained at the maximum allowed value of $\alpha_{12} = 0.32$ by the perturbative unitarity conditions discussed in Sec. IV.

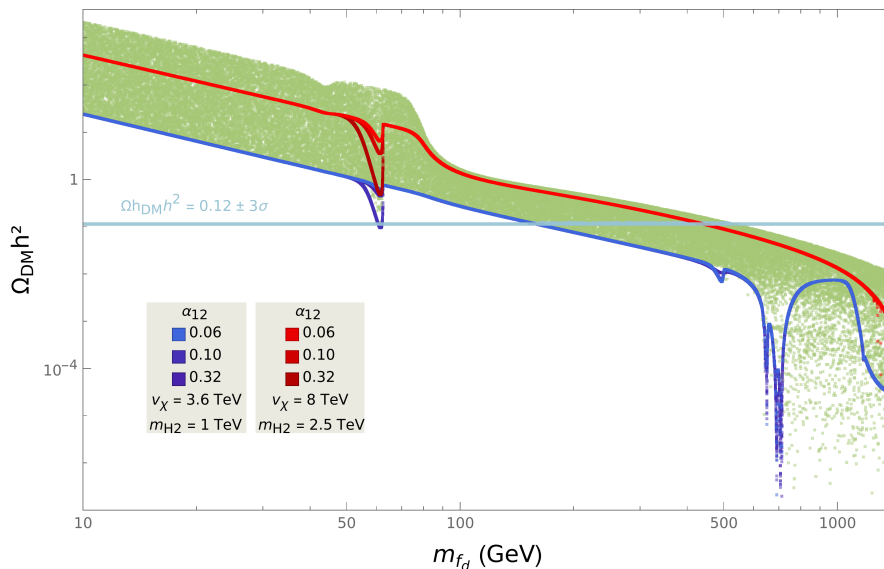


FIG. 4. In green, we show the relic density versus DM mass for a random scan. The colored lines represent the scenarios for fixed values of $\alpha_{13} = 0.003$, $\alpha_{23} = 0.03$, and $m_{S_d} = 5 \text{ TeV}$. The values of the parameters v_χ , α_{12} , and m_{H_2} are shown in the plot. The horizontal light blue line indicates the Planck 3σ range. Random values for the parameters were considered to explore how α_{12} and v_χ influence the Higgs resonance (first dip around 62.5 GeV), the H_2 resonance (second dip around 500 GeV), and the Z' resonance (around 1 TeV).

Another important set of constraints on DM candidates comes from contemporary direct detection experiments [55, 56], which aim to detect WIMP DM by measuring the kinetic energy transferred to a nucleus during its interaction with a DM particle. These experiments have established upper bounds on the WIMP-nucleus scattering cross section. In general, WIMP-nucleus interactions are classified as either spin-independent (SI) or spin-dependent (SD). Currently, the most stringent limit for spin-independent scattering is set at $36 \text{ GeV}/c^2$, rejecting cross sections above $9.2 \times 10^{-48} \text{ cm}^2$ at the 90% confidence level, as reported by the LUX-ZEPLIN (LZ) collaboration [55]. In this work, we analyze the DM candidate f_d and find that spin-independent (SI) interactions dominate. Using the MicrOMEGAs package, we compute the SI elastic scattering cross section per nucleon, $\sigma_{\text{SI-nucleon}}$, for the parameter region that satisfies the relic density constraint. This region is highlighted in light blue in Fig. 5. Additionally, we present the sensitivity curves for the LZ [55] and PandaX-4T experiments [56], along with the projected sensitivity curves for the near-future XLZD [57] and PandaX-xT [58] experiments, shown as dashed lines.

For the parameter space that satisfies the correct DM relic density, the model includes a small region that has already been excluded (including the region at the Higgs resonance, which is largely ruled out)

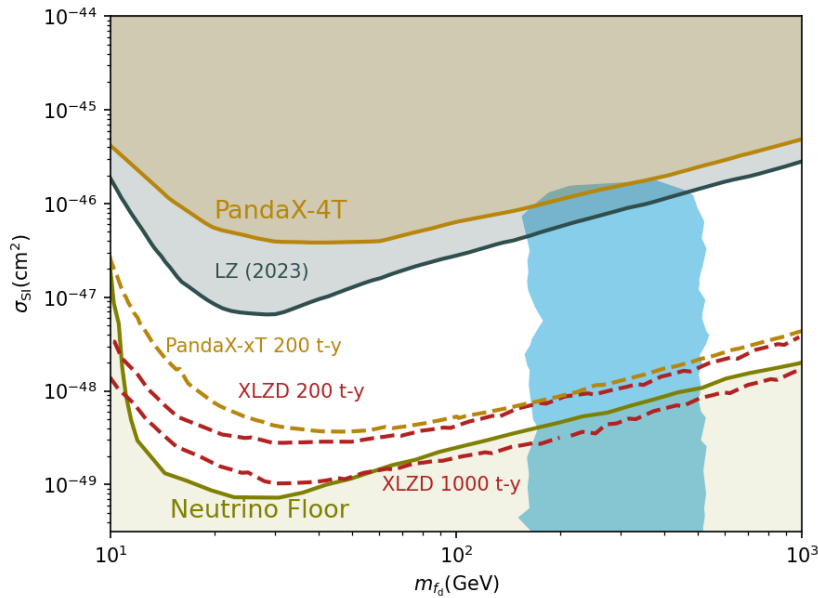


FIG. 5. The direct detection cross section versus DM mass for the parameter region that satisfies the correct relic density is shown in light blue. Also displayed are the sensitivity curves for the LZ [55] and PandaX-4T [56] experiments, as well as the projected sensitivity curves for the near-future XLZD [57] and PandaX-xT [58] experiments (dashed lines). Additionally, the updated definition of the neutrino floor from 2021 [59] is included.

and another that is near the sensitivity of current experimental searches. Moreover, the model predicts a significant parameter space located deep within the neutrino floor region [59]. SD interactions are not considered in this analysis, as they are, in this model, several orders of magnitude weaker than the current experimental constraints on SD scattering.

IX. CONCLUSIONS

In this work, we propose a scale-invariant model based on the gauge group $SU(3)_C \otimes SU(3)_L \otimes U(1)_X \otimes U(1)_N$, with the $U(1)_N$ symmetry chosen such that a natural P_M discrete symmetry emerges after the dynamical symmetry breaking. As part of the 3-3-1 family, this construction has the potential to tackle several unresolved challenges of the SM, such as the origin of neutrino masses, the determination of the number of lepton and quark families, and the nature of dark matter.

One of the significant advances of the proposed framework is the reduction in the number of scalar

fields in high representations of the gauge group, simplifying the scalar potential while preserving the ability to break the gauge symmetry to $SU(3)_C \otimes U(1)_Q$. This optimized scalar sector, combined with the imposition of scale invariance, enhances predictability compared to earlier 3-3-1 constructions, which often suffered from excessive scalar complexity. In Sec. III, we analyze the scalar sector in detail, following the Gildener-Weinberg approximation, and demonstrate that, in addition to the SM-like Higgs, H_1 , and the dilaton, H_4 , the model contains two CP-even scalars, $H_{2,3}$, and one complex scalar, S_d .

We found that the perturbative unitarity constraints, discussed in Sec. IV, impose critical bounds on the quartic couplings and other parameters of the model, ensuring the theoretical consistency of the framework. By analyzing two-to-two scattering amplitudes at high energy, we derived explicit conditions that all quartic couplings and eigenvalues of the scalar coupling matrix must satisfy. These constraints play a vital role in limiting the parameter space, directly influencing the scalar masses, mixing angles, and VEVs within the model. In particular, these conditions require the mixing angles α_{12} , α_{13} , and α_{23} to be small (see Eq. (85)).

Furthermore, in analogy to Ref. [20], the introduction of vector-like quarks and leptons, together with a natural choice of the different VEVs, partially addresses the hierarchy among the charged lepton and quark masses through a universal see-saw mechanism, facilitating the generation of masses for all SM particles as well as new exotic states at energy scales compatible with scale invariance. This framework surpasses the model proposed in Ref. [20], as it also provides an explanation for the hierarchy among the charged lepton masses, as shown in Sec. VI. Charged lepton flavor-violating effects are present in the model due to mixing between SM charged leptons and the exotic leptons. For scalar mediated charged lepton flavor-violating processes the constraints are avoided due to heavy mass of exotic particles, as well as relations between the couplings due to seesaw mechanism. The gauge mediated charged lepton flavor-violating processes, on the other hand, are avoided due to small couplings.

The gauge sector in the scale-invariant 3-3-1-1 model, treated in Sec. V, features a rich structure derived from the kinetic terms of the scalar bosons and their interactions with the gauge bosons. The charged (non-Hermitian) bosons arise from the non-diagonal generators of $SU(3)_L$ and acquire masses proportional to v_η (which in this model is equal to v_{SM}) in the case of W^\pm , and proportional to the 3-3-1 energy scale, v_χ . In the neutral boson sector, mixing among gauge fields produces four physical states: the massless photon and the Z , Z' , and Z'' bosons, whose masses are linked to the VEVs of the η , χ , and σ fields. Among these, the Z'' boson is particularly important as it stabilizes the scalar potential, enabling dynamical symmetry breaking and ensuring the model's theoretical consistency at high energy

scales. Furthermore, experimental bounds on the ρ_0 parameter, which measures the ratio of W^\pm and Z boson masses, impose a lower limit on the $SU(3)_L$ symmetry-breaking scale, $v_\chi \gtrsim 3.6 \text{ TeV}$. This result underscores the model's compatibility with current data and its potential for future experimental validation.

A key strength of the proposed model lies in its ability to naturally explain dark matter phenomenology. The model incorporates a dark matter candidate stabilized due to the P_M symmetry, which emerges after symmetry breaking. Among the possible P_M -odd neutral particles, the fermion f_d is identified as a viable dark matter candidate. Our analysis shows that f_d satisfies the relic density constraint within the mass range $160 \text{ GeV} \lesssim m_{f_d} \lesssim 520 \text{ GeV}$, as well as in the Higgs resonance, as shown in Fig. 5. This result primarily depends on the scalar mixing parameters $\alpha_{12}, \alpha_{13}, \alpha_{23}$ and the VEVs v_χ, v_σ, v_ϕ (see Fig. 4). Spin-independent scattering cross-sections for f_d are consistent with experimental limits from LZ and PandaX-4T in certain regions of the parameter space but exclude the Higgs resonance. Moreover, some parts of the parameter space lie below the neutrino floor, making them inaccessible to current detection technologies.

Other dark matter candidates, such as the vector boson V^0 and the scalar S_d , are excluded due to their instability or incompatibility with direct detection constraints. Furthermore, a substantial portion of the parameter space can be probed in upcoming experiments, such as XLZD and PandaX-xT, offering opportunities for further validation of the model's predictions.

ACKNOWLEDGMENTS

We would like to thank Y. Villamizar, Y. Porto, J. P. Carvalho-Correa, and A. C. D. Viglioni for discussions. This work was supported by the Estonian Research Council grants PRG803, TEM-TA23, RVTT3 and RVTT7, and the Center of Excellence program TK202 'Fundamental Universe'. This study was also financed, in part, by the São Paulo Research Foundation (FAPESP), Brasil, process numbers 2022/10785-4, and 2023/13275-0. B. L. Sánchez-Vega thanks the National Council for Scientific and Technological Development of Brazil, CNPq, for the financial support through grant n° 311699/2020-0. We dedicate this work to the memory of Alex G. Dias, an esteemed colleague and dear friend, whose contributions to science and kindness deeply impacted those who worked alongside him. His legacy will continue to inspire us and future generations.

-
- [1] M. Singer, J. W. F. Valle, and J. Schechter, *Phys. Rev.* **D22**, 738 (1980).
 - [2] F. Pisano and V. Pleitez, *Phys. Rev.* **D46**, 410 (1992), [arXiv:hep-ph/9206242 \[hep-ph\]](#).
 - [3] R. Foot, O. F. Hernandez, F. Pisano, and V. Pleitez, *Phys. Rev. D* **47**, 4158 (1993), [arXiv:hep-ph/9207264](#).
 - [4] P. H. Frampton, *Phys. Rev. Lett.* **69**, 2889 (1992).
 - [5] J. C. Montero, F. Pisano, and V. Pleitez, *Phys. Rev.* **D47**, 2918 (1993), [arXiv:hep-ph/9212271 \[hep-ph\]](#).
 - [6] V. Pleitez and M. D. Tonasse, *Phys. Rev. D* **48**, 2353 (1993), [arXiv:hep-ph/9301232](#).
 - [7] R. Foot, H. N. Long, and T. A. Tran, *Phys. Rev.* **D50**, R34 (1994), [arXiv:hep-ph/9402243 \[hep-ph\]](#).
 - [8] V. Pleitez, *Phys. Rev. D* **53**, 514 (1996), [arXiv:hep-ph/9412304](#).
 - [9] M. Ozer, *Phys. Rev. D* **54**, 1143 (1996).
 - [10] H. N. Long, *Phys. Rev.* **D53**, 437 (1996), [arXiv:hep-ph/9504274 \[hep-ph\]](#).
 - [11] J. C. Montero and B. L. Sánchez-Vega, *Phys. Rev.* **D84**, 055019 (2011), [arXiv:1102.5374 \[hep-ph\]](#).
 - [12] P. V. Dong, H. T. Hung, and T. D. Tham, *Phys. Rev. D* **87**, 115003 (2013), [arXiv:1305.0369 \[hep-ph\]](#).
 - [13] P. V. Dong, *Phys. Rev. D* **92**, 055026 (2015), [arXiv:1505.06469 \[hep-ph\]](#).
 - [14] A. Alves, G. Arcadi, P. V. Dong, L. Duarte, F. S. Queiroz, and J. W. F. Valle, *Phys. Lett. B* **772**, 825 (2017), [arXiv:1612.04383 \[hep-ph\]](#).
 - [15] J. Leite, O. Popov, R. Srivastava, and J. W. F. Valle, *Phys. Lett. B* **802**, 135254 (2019), [arXiv:1909.06386 \[hep-ph\]](#).
 - [16] J. Leite, A. Morales, J. W. F. Valle, and C. A. Vaquera-Araujo, *Phys. Rev. D* **102**, 015022 (2020), [arXiv:2005.03600 \[hep-ph\]](#).
 - [17] J. C. Montero, A. Romero, and B. L. Sánchez-Vega, *Phys. Rev. D* **97**, 063015 (2018), [arXiv:1709.04535 \[hep-ph\]](#).
 - [18] G. C. Branco, P. M. Ferreira, L. Lavoura, M. N. Rebelo, M. Sher, and J. P. Silva, *Phys. Rept.* **516**, 1 (2012), [arXiv:1106.0034 \[hep-ph\]](#).
 - [19] S. P. Martin, *Adv. Ser. Direct. High Energy Phys.* **18**, 1 (1998), [arXiv:hep-ph/9709356](#).
 - [20] A. G. Dias, J. Leite, and B. L. Sánchez-Vega, *Phys. Rev. D* **106**, 115008 (2022), [arXiv:2207.06276 \[hep-ph\]](#).
 - [21] S. R. Coleman and E. J. Weinberg, *Phys. Rev.* **D7**, 1888 (1973).
 - [22] E. Gildener and S. Weinberg, *Phys. Rev.* **D13**, 3333 (1976).
 - [23] J. C. Montero and B. L. Sánchez-Vega, *Phys. Rev.* **D91**, 037302 (2015), [arXiv:1411.2580 \[hep-ph\]](#).
 - [24] A. Davidson and K. C. Wali, *Phys. Rev. Lett.* **59**, 393 (1987).
 - [25] S. Dimopoulos and H. Georgi, *Nucl. Phys. B* **193**, 150 (1981).
 - [26] G. R. Farrar and P. Fayet, *Phys. Lett. B* **76**, 575 (1978).
 - [27] L. E. Ibanez and G. G. Ross, *Nucl. Phys. B* **368**, 3 (1992).

- [28] M. Kadastik, K. Kannike, and M. Raidal, *Phys. Rev. D* **80**, 085020 (2009), [Erratum: *Phys.Rev.D* 81, 029903 (2010)], [arXiv:0907.1894 \[hep-ph\]](#).
- [29] M. Kadastik, K. Kannike, and M. Raidal, *Phys. Rev. D* **81**, 015002 (2010), [arXiv:0903.2475 \[hep-ph\]](#).
- [30] P. V. Dong, D. T. Huong, F. S. Queiroz, and N. Thuy, *Phys. Rev. D* **90**, 075021 (2014), [arXiv:1405.2591 \[hep-ph\]](#).
- [31] M. Gell-Mann, P. Ramond, and R. Slansky, in *Supergravity*, edited by P. v. Niuwenhuizen and D. Freedman (North Holland Publ. Co., 1979).
- [32] T. Yanagida, in *Proceedings of the Workshop on the Baryon Number of the Universe and Unified Theories*, edited by O. Sawada and A. Sugamoto (Tsukuba, Japan, 1979).
- [33] R. N. Mohapatra and G. Senjanovic, *Phys. Rev. Lett.* **44**, 912 (1980).
- [34] S. L. Glashow, NATO Adv. Study Inst. Ser. B Phys. **59**, 687 (1980).
- [35] P. Minkowski, *Phys. Lett.* **B67**, 421 (1977).
- [36] K. Kannike, A. Kubarski, and L. Marzola, *Phys. Rev.* **D99**, 115034 (2019), [arXiv:1904.07867 \[hep-ph\]](#).
- [37] L. Alexander-Nunneley and A. Pilaftsis, *JHEP* **09**, 021 (2010), [arXiv:1006.5916 \[hep-ph\]](#).
- [38] H. Fritzsch and J. Plankl, *Phys. Rev. D* **35**, 1732 (1987).
- [39] B. Singh Koranga and V. K. Nautiyal, *Int. J. Theor. Phys.* **60**, 781 (2021).
- [40] K. Kannike, *Journal of High Energy Physics* **2024** (2024), [10.1007/jhep01\(2024\)176](#).
- [41] S. Navas *et al.* (Particle Data Group), *Phys. Rev. D* **110**, 030001 (2024).
- [42] R. L. Workman *et al.* (Particle Data Group), *PTEP* **2022**, 083C01 (2022).
- [43] W. Grimus and L. Lavoura, *JHEP* **11**, 042 (2000), [arXiv:hep-ph/0008179 \[hep-ph\]](#).
- [44] J. Casas and A. Ibarra, *Nuclear Physics B* **618**, 171–204 (2001).
- [45] T. J. Kärkkäinen and Z. Trócsányi, *J. Phys. G* **49**, 045004 (2022), [arXiv:2105.13360 \[hep-ph\]](#).
- [46] I. Esteban, M. C. Gonzalez-Garcia, M. Maltoni, I. Martinez-Soler, J. P. Pinheiro, and T. Schwetz, “Nufit-6.0: Updated global analysis of three-flavor neutrino oscillations,” (2024), [arXiv:2410.05380 \[hep-ph\]](#).
- [47] CMS Collaboration, *CERN Reports* (2019).
- [48] N. Aghanim, Y. Akrami, M. Ashdown, *et al.*, *Astronomy & Astrophysics* **641**, A6 (2020).
- [49] P. Gondolo and G. Gelmini, *Nuclear Physics B* **360**, 145 (1991).
- [50] K. Griest and D. Seckel, *Phys. Rev. D* **43**, 3191 (1991).
- [51] A. Alloul, N. D. Christensen, C. Degrande, C. Duhr, and B. Fuks, *Computer Physics Communications* **185**, 2250 (2014).
- [52] Q.-H. Cao and D.-M. Zhang, “Collider phenomenology of the 3-3-1 model,” (2016), [arXiv:1611.09337 \[hep-ph\]](#).
- [53] A. Belyaev, N. D. Christensen, and A. Pukhov, *Computer Physics Communications* **184**, 1729 (2013).
- [54] G. Alguero, G. Bélanger, F. Boudjema, S. Chakraborti, A. Goudelis, S. Kraml, A. Mjallal, and A. Pukhov, *Computer Physics Communications* **299**, 109133 (2024).
- [55] J. Aalbers *et al.* (LUX-ZEPLIN Collaboration), *Phys. Rev. Lett.* **131**, 041002 (2023).

- [56] Y. Meng *et al.* (PandaX-4T Collaboration), *Phys. Rev. Lett.* **127**, 261802 (2021).
- [57] J. Aalbers *et al.*, *Journal of Physics G: Nuclear and Particle Physics* **50**, 013001 (2022).
- [58] A. Abdukerim *et al.*, *Science China Physics, Mechanics & Astronomy* **68** (2024), 10.1007/s11433-024-2539-y.
- [59] C. A. J. O'Hare, *Physical Review Letters* **127** (2021), 10.1103/physrevlett.127.251802.